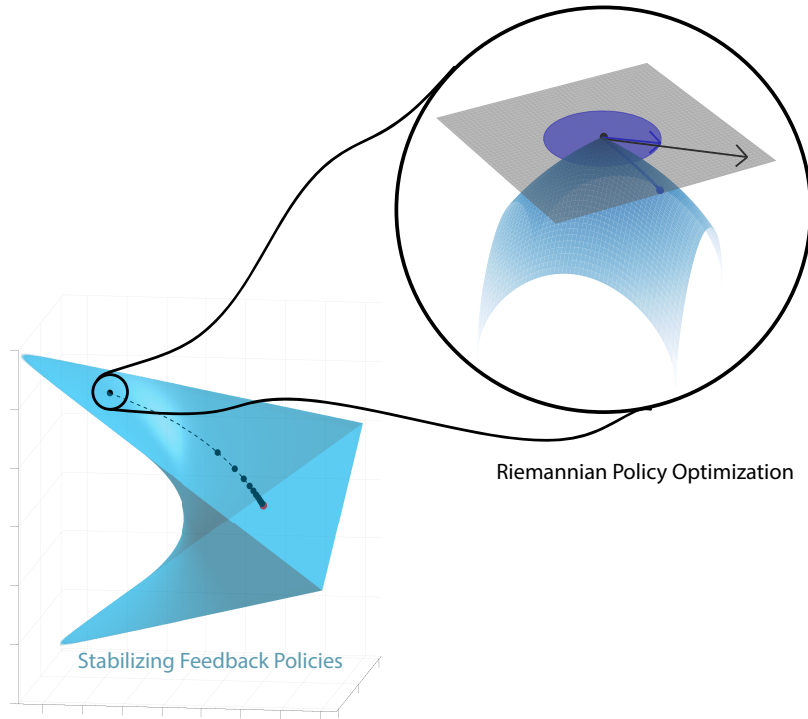


Graphical Abstract

Policy Optimization in Control: Geometry and Algorithmic Implications

Shahriar Talebi, Yang Zheng, Spencer Kraisler, Na Li, Mehran Mesbahi



The article surveys geometric aspects of stabilizing feedback control in the context of policy optimization for iconic synthesis problems, including LQR, LQG, and \mathcal{H}_∞ .

Highlights

Policy Optimization in Control: Geometry and Algorithmic Implications

Shahriar Talebi, Yang Zheng, Spencer Kraisler, Na Li, Mehran Mesbahi

- Policy optimization (PO) provides a unified perspective on feedback design subject to stabilization constraint,
- PO also provides a bridge between control theory and data-driven design techniques such as model-free reinforcement learning,
- Geometric properties of the set of stabilizing feedback gains and how their interact with various performance measures become of out most importance while designing PO-based algorithms,
- PO highlights design and algorithmic challenges in control engineering beyond classic paradigms involving quadratic costs and linear dynamics.

Policy Optimization in Control: Geometry and Algorithmic Implications

Shahriar Talebi^a, Yang Zheng^b, Spencer Kraisler^c, Na Li^a, Mehran Mesbahi^c

^a*Harvard University, School of Engineering and Applied Sciences,
150 Western Ave, Boston, 02134, MA, US*

^b*University of California San Diego, Department of Electrical and Computer Engineering,
9500 Gilman Drive, La Jolla, 92093, CA, US*

^c*University of Washington, Department of Aeronautics and Astronautics,
3940 Benton Ln NE, Seattle, 98195, WA, US*

Abstract

This survey explores the geometric perspective on policy optimization within the realm of feedback control systems, emphasizing the intrinsic relationship between control design and optimization. By adopting a geometric viewpoint, we aim to provide a nuanced understanding of how various “complete parameterization”—referring to the policy parameters together with its Riemannian geometry—of control design problems, influence stability and performance of local search algorithms. The paper is structured to address key themes such as policy parameterization, the topology and geometry of stabilizing policies, and their implications for various (non-convex) dynamic performance measures. We focus on a few iconic control design problems, including the Linear Quadratic Regulator (LQR), Linear Quadratic Gaussian (LQG) control, and \mathcal{H}_∞ control. In particular, we first discuss the topology and Riemannian geometry of stabilizing policies, distinguishing between their static and dynamic realizations. Expanding on this geometric perspective, we then explore structural properties of the aforementioned performance measures and their interplay with the geometry of stabilizing policies in presence of policy constraints; along the way, we address issues such as spurious stationary points, symmetries of dynamic feedback policies, and (non-)smoothness of the corresponding performance measures. We conclude the survey with algorithmic implications of policy optimization in feedback design.

Keywords: Benign nonconvexity, Global Optimality, Geometry of Stabilizing Policies, \mathcal{H}_∞ Robust Control, Linear Quadratic Gaussian (LQG), Linear Quadratic Regulator (LQR), Output and Structured LQR, Optimal Control, Policy Optimization Algorithms, Riemannian Geometry and Optimization

Contents

1	Introduction	3
2	Policy Optimization in Control: the Role of Parameterization	4
2.1	Policy Parameterization for Closed-loop Optimal Control	5
2.2	Policy Optimization for Iconic Optimal and Robust Control Problems	6
2.2.1	LQR under Static State-feedback Policies	6
2.2.2	LQG under Dynamic Output-feedback Policies	7
2.2.3	\mathcal{H}_∞ -robust Control under Static State-feedback Policies	8

3	Topology and Geometry of Stabilizing Policies	9
3.1	Riemannian Geometry of Stabilizing Policies	9
3.2	Topology and Geometry of Dynamic Output-feedback Polices	11
3.3	Symmetries of Dynamic Output-feedback Policies: a Quotient Geometry	12
4	Geometry of Performance Objectives on Stabilizing Policies	14
4.1	Riemannian Geometry and Policy Optimization	14
4.2	Stability Certificate for the Euclidean Retraction	16
4.3	Linear Quadratic Regulator (LQR)	17
4.3.1	Unconstrained Case	17
4.3.2	Linearly Constrained Case	18
4.4	Linear Quadratic Gaussian (LQG) Control	19
4.4.1	Spurious Stationary Points and Global Optimality	20
4.4.2	Invariances of LQG: a Quotient Geometry	21
4.5	\mathcal{H}_∞ -norm: Systems with Adversarial Noise	23
5	Algorithmic Implications	25
5.1	Convergence of Policy Optimization Algorithms	25
5.2	Oracle-based Data-driven Algorithms	27
5.3	Optimal Estimation Problems	28
5.4	Broader Implications: Iterative Learning Procedures	29
6	Summary and Outlook	29
7	Notes and Commentary	29
8	Acknowledgements	30

1. Introduction

Optimization and control have had a rich symbiotic relationship since their inception. This is not surprising as the current dominant perspective on control design highlights: the design process for a dynamic system involves formalizing the notion of “best” with respect to selectable system parameters¹—followed by devising algorithms that optimize the design objective with respect to these parameters. The interactions between these two disciplines has highlighted a crucial aspect of control design: identifying design objectives that, with respect to a given parameterization of control system (or more generally, parameters in the overall design architecture), facilitate algorithmic developments while maintaining sound engineering judgment. For example, it is common to see a family of solution strategies for a given control design problem, including open vs. closed-loop, approaches based on variational (Liberzon, 2011) or dynamic programming (Bertsekas, 2012), and constructs such as co-state, value, and, of course, *policy* (Bertsekas, 2011, 2017). Each of these formalisms offer insights into control design, that although in principle can be formalized as an optimization problem, but reflect distinct intricacies in designing systems that evolve over time, interact with their environments, and have memory. For example, system theoretic properties such as stability, minimality, and robustness, significantly “spice up” not only the control design problem formulation but also the adopted strategies for their solution (Zabczyk, 2020; Sontag, 2013).

A powerful abstraction in this plethora of design techniques is that of *policy*, mapping what the system has observably done to what can influence its subsequent behavior. Not only does the existence of an “optimal” policy reduce the complexity of control implementation (as the control input is a trajectory) at the expense of realizing feedback, but as it turns out, it also addresses one of the key features of control design, namely robustness (Skogestad and Postlethwaite, 2005; Doyle et al., 2013). This survey aims to capture the *geometry* of policy optimization for a few iconic design techniques in control (including stabilization, linear quadratic control, and \mathcal{H}_∞ robust control), capturing distinct facets of adopting such a perspective for feedback design. However, as we undertake such an endeavor, it is important to comment on the timeliness of this approach, as well as how it connects—and is distinct—from previous works, particularly in relation to its reference to “geometry”.

Historically, the “geometric” qualifier has been used in systems and control to shed light on more subtle aspects of system design. In linear geometric control, subspace geometry is used to delineate the coordinate-independence of system theoretic constructs such as controllability and observability (Wonham, 1985; Trentelman et al., 2001). Geometric nonlinear control, on the other hand, characterizes notions such as controllability for nonlinear systems, by viewing their evolution in terms of vector fields, and then brings forth a differential geometric formalism for their analysis, e.g., differentiable manifold, distributions, and Lie algebras (Isidori, 2013; Nijmeijer and Schaft, 1990); the aim is to free control theory (analysis and synthesis) from the confinements of linearity and linear algebra via a coordinate-free analysis of dynamical systems. Using this geometric vista, linear maps are uplifted to diffeomorphisms, while notions such as controllability matrix are revealed as Lie brackets (Brockett, 2014). As these two examples demonstrate, “geometry” is often used to hint at coordinate-independence of concepts, similar to how finite dimensional vector spaces are related to linear algebra. Other notable works in adopting a geometric perspective in systems and control theory, particularly in relation to realization theory and system identification include (Hazewinkel and Kalman, 1976; Hazewinkel, 1980; Tannenbaum, 1981).

¹Whatever the “best” qualifier implies.

By including “geometry” in the title of this survey, we deliberately mean to promote adopting a similar geometric perspective as the aforementioned works, but for the space of feedback control policies rather than system models or their trajectories, which highlights the importance of how one characterizes notions such as distance and direction for these policies. Such a perspective not only complements other features of this space (in addition to its topological, analytic, or algebraic structures) but more importantly, has direct consequences for devising algorithms for the corresponding optimization problems. This geometric perspective and its algorithmic implications have also been adopted in neighboring decision sciences, e.g., statistical learning and Markov Decision Processes (MDPs). Notable in the landscape of such geometric techniques, we mention the notion of natural gradients, where the geometry of the underlying model, singled out in the design objective, is systematically used to synthesize algorithms that behave invariant under certain re-parameterizations. By invariance, we mean embedding the underlying model with a notion of distance that is preserved under certain mappings, e.g., Fisher metric in statistical learning (Amari, 1998, 2016). Closely related to the present survey is adopting the theory of natural gradients for MDPs as first proposed in (Kakade, 2002), where the Hessian geometry induced by the entropy plays a central role in the design and convergence analysis of the corresponding algorithms; also see (Agarwal et al., 2021).

These geometric insights have a number of algorithmic and system-theoretic consequences. For example, as we will see, improving the policy by taking steps in the direction of its (negative) gradient proves to be an effective means of obtaining optimal policies, i.e., first-order policy updates. The “zeroth” order version of the above scheme, on the other hand, leads to using function evaluations to approximate the corresponding gradients from data—say, when such evaluations can be obtained from an oracle that can return approximate values of the cost, closely relates to reinforcement learning setup. Key questions in this data-driven realization of geometric first-order methods are with how many function evaluations (and with what accuracy) and over how many iterations, an accurate estimate of the optimal policy can be obtained (Fazel et al., 2018b; Malik et al., 2019; Mohammadi et al., 2021a, 2020). Furthermore, these concepts resonate with optimal estimation problems due to the profound duality relation between control and estimation (Talebi et al., 2023).

The survey is structured as follows. In §2 we make the parameterization theme on control design alluded to above more explicit. While this perspective provides a direct approach to formalize policy optimization for control, it also underscores how the constraints imposed by system theoretic notions such as stabilizability make the feasible set of the optimization non-trivial. This is first more pursued for static feedback, followed by that of dynamic feedback policies in §3. We then turn our attention to how distinct design performance measures interact with the feasible set of feedback policies in §4. Algorithmic implications and data-driven realizations of the geometric perspective on policy optimization are then examined under §5. In §6, we provide a summary of the key points put forth by this survey as well as our outlook on the future work; §7 provides commentary on references with contributions reflected in this survey.

2. Policy Optimization in Control: the Role of Parameterization

Let us consider a discrete-time dynamical system:

$$x_{t+1} = f(x_t, u_t, w_t), \quad y_t = h(x_t, w_t), \quad (1)$$

where $x_t \in \mathbb{R}^n$ is the system state, $u_t \in \mathbb{R}^m$ is the control input, and $y_t \in \mathbb{R}^p$ is the system measurement. We refer to w_t as the exogenous signal, representing unmodeled dynamics, stochastic

noise, or disturbances. At each time step t , we use $l(x_t, u_t)$ to denote the stage cost as a function of the current state and input. The goal of infinite-horizon optimal control is to choose $\mathbf{u} = (u_0, u_1, \dots)$ to minimize an accumulated cost over the infinite time horizon. More formally, we define the T -stage accumulated cost as

$$J_T(\mathbf{u}, \mathbf{w}, x_0) := \sum_{t=0}^T l(x_t, u_t), \quad (2)$$

where $\mathbf{w} = (w_0, w_1, \dots)$. The cost (2) highlights that the implicit state trajectory \mathbf{x} depends on the control input \mathbf{u} , the exogenous input \mathbf{w} , and initial state x_0 . Often \mathbf{w} and x_0 are modeled either stochastically or deterministically, and the performance of the closed-loop system is measured based on the corresponding average or worst case performance. An example of such infinite-horizon control performance is

$$J(\mathbf{u}) := \lim_{T \rightarrow \infty} \mathbb{E}_{\mathbf{w}, x_0} \frac{1}{T} J_T(\mathbf{u}, \mathbf{w}, x_0), \quad (3)$$

which presumes stochastic exogenous input \mathbf{w} and initial state x_0 (by expectation with respect to statistical properties of \mathbf{w} and x_0); as in the formulation of LQR and LQG costs. On the other hand, when the exogenous inputs are adversarial, one may replace the expectation with respect to \mathbf{w} with the worst-case performance assuming bounded energy for \mathbf{w} ; as in the formulation of \mathcal{H}_∞ cost.

2.1. Policy Parameterization for Closed-loop Optimal Control

Instead of optimizing over the input sequence \mathbf{u} in (3), which we refer to as the *optimal open-loop control design*, we consider instead optimizing over a class of *feedback policies* that act on the system history $\mathcal{H}_t := (u_{0:t-1}, y_{0:t})$, where $u_{0:t-1} := (u_0, u_1, \dots, u_{t-1})$ and similar for $y_{0:t}$. As such a *feedback* or *closed-loop policy* at time t , denoted by $\pi_t : \mathcal{H}_t \mapsto u_t$, is a measurable function that maps the system history \mathcal{H}_t at time t to a control input u_t . We can alternatively define $\pi_t(\mathcal{H}_t)$ to be a distribution and set $u_t \sim \pi_t(\mathcal{H}_t)$.² We will call $\pi = (\pi_0, \pi_1, \dots)$ the feedback policy; for brevity, we will often write $\pi(\mathcal{H}_t) := \pi_t(\mathcal{H}_t)$. Let Π be the infinite-dimensional vector space of all such feedback policies $\pi(\cdot)$. Then, the optimal closed-loop policy problem reads as

$$\min_{\pi \in \Pi} J(\mathbf{u}) \quad (4a)$$

$$\text{subject to } (1), u_t = \pi(\mathcal{H}_t). \quad (4b)$$

Since it is non-trivial to optimize directly over this space Π , the so-called “policy parameterization” approach is to parameterize (a subset of) Π with some d -dimensional set of parameters $\theta \in \Theta \subset \mathbb{R}^d$. That way, our parameterized family of policies $\{\pi_\theta(\cdot)\}_{\theta \in \Theta} \subset \Pi$ is finite-dimensional. Note that policy parameterization is rather flexible, as it can represent linear dynamical systems, polynomials, kernels, or neural networks. In some important cases, one can restrict the class of policies under consideration without loss of generality. For instance, it is known that static/dynamic “linear policies” are sufficient for optimal and robust control problems posed for linear time-invariant (LTI) systems (Zhou et al., 1996). With policy parameterization, (4) is reduced to the optimal closed-loop parameterized policy problem:

²In this case, we would have to slightly augment (3).

$$\min_{\theta \in \Theta} J(\theta) := J(\pi_\theta(\mathcal{H})), \quad (5)$$

where $\pi_\theta(\mathcal{H})$ denotes the input signal obtained as $\mathbf{u} = (\pi_\theta(\mathcal{H}_0), \pi_\theta(\mathcal{H}_1), \dots)$. If π^* solves (4) and θ^* solves (5) then it should be remarked $J(\pi^*) \leq J(\pi_{\theta^*})$, with equality if and only if the parameterization is “rich enough,” e.g., static and dynamic linear feedback policies for LQR and LQG problems, respectively. Further, we can explicitly incorporate a policy constraint on Θ that represents closed-loop stability or an information structure required for control synthesis.

Conceptually, it appears simple and flexible to use local search algorithms, such as policy gradient or its variants, to seek the “best” policy in (5). Once the corresponding cost in (5) can be estimated from sampled trajectories, this policy optimization setup indeed is very amenable for data-driven design paradigms such as reinforcement learning (Recht, 2019). One goal of this article is to highlight some *rich* and *intriguing*, geometry in policy optimization (5), including nonconvexity, potentially disconnected feasible domain Θ , spurious stationary points of the cost J , symmetry, and smooth (Riemannian) manifold structures. Our focus will be on classic control tasks for LTI systems including LQR, LQG, and \mathcal{H}_∞ robust control. These geometrical understandings will often provide insights for designing principled local search algorithms to solve (5), such as policy gradient methods with global/local convergence guarantees (Fazel et al., 2018a; Bu et al., 2019; Mohammadi et al., 2021c; Hu et al., 2023). Inspired by the rich geometry in (5), we will further emphasize that a “complete policy parameterization” should come with an associated metric, capturing the inherent geometry, which may help improve the problem’s conditioning (Talebi and Mesbahi, 2022; Kraiser and Mesbahi, 2024).

2.2. Policy Optimization for Iconic Optimal and Robust Control Problems

2.2.1. LQR under Static State-feedback Policies

For the LQR problem, the system dynamics (1) read as

$$x_{t+1} = Ax_t + Bu_t + w_t, \quad y_t = x_t, \quad (6)$$

where the process noise is white and Gaussian $w_t \sim \mathcal{N}(0, \Sigma)$ for some $\Sigma \succ 0$. Since the state is directly observed, the system history takes the form $\mathcal{H}_t = (u_{0:t-1}, x_{0:t})$. Given the performance weighting matrices $Q \succeq 0, R \succ 0$, (4) reduces to the optimal LQR problem:

$$\min_{\pi \in \Pi} J_{\text{LQR}}(\mathbf{u}) := \lim_{T \rightarrow \infty} \mathbb{E}_{\mathbf{w}, x_0} \frac{1}{T} J_T(\mathbf{u}, \mathbf{w}, x_0) \quad (7a)$$

$$\text{subject to} \quad (6), u_t = \pi(\mathcal{H}_t) \quad (7b)$$

with the quadratic stage cost $l(x_t, u_t) = \frac{1}{2}(x_t^T Q x_t + u_t^T R u_t)$. Note that the cost in (7) will be oblivious to any bounded initial condition x_0 as long as the policy is stabilizing, and the Gaussian assumption on noise can be lifted.

Alternatively, when the dynamics is noiseless but the initial condition is uncertain, we might be interested in minimizing the following objective instead

$$\min_{\pi \in \Pi} J_{\text{LQR}}(\mathbf{u}) := \lim_{T \rightarrow \infty} \mathbb{E}_{x_0} J_T(\mathbf{u}, \mathbf{0}, x_0) \quad (8a)$$

$$\text{subject to} \quad (6), u_t = \pi(\mathcal{H}_t) \quad (8b)$$

where x_0 is drawn from a distribution with covariance $\Sigma \succ 0$. We will see later that both of the problems in (7) and (8) essentially amount to the same policy optimization problem.

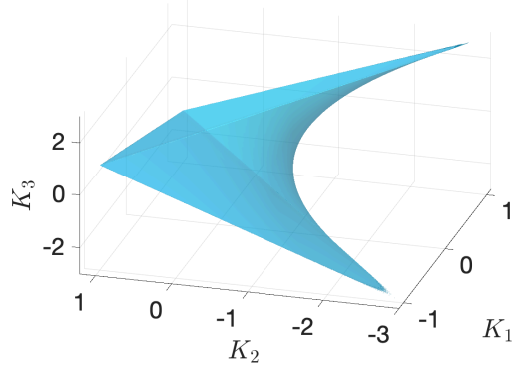


Figure 1: The non-convex set of stabilizing static state-feedback policies \mathcal{S} for $A = \begin{bmatrix} 0 & 1 & 0 \\ 0 & 0 & 1 \\ 0 & 0 & 0 \end{bmatrix}$ and $B = \begin{bmatrix} 0 \\ 0 \\ 1 \end{bmatrix}$.

A remarkable property of the closed-loop optimal LQR problem is that the optimal policy π^* , when exists, is linear in the states and depends only on the current states. That is, $\pi^*(\mathcal{H}_t) = \pi^*(x_t) = Kx_t$ for some $K \in \mathbb{R}^{m \times n}$ (Anderson and Moore, 2007). Inspired by this property, for both (7) and (8), we can parameterize the LQR policy as a linear mapping $x_t \mapsto u_t = Kx_t$ and referred to as policy K for simplicity. Then, the set of static stabilizing state-feedback policies is

$$\Theta := \mathcal{S} = \{K \in \mathbb{R}^{m \times n} : \rho(A + BK) < 1\}. \quad (9)$$

where $\rho(\cdot)$ denotes the spectral radius of a square matrix. Following (5), we can define J_{LQR} over \mathcal{S} , where $J_{\text{LQR}}(K)$ corresponds to the objective in either (7) or (8). Our parameterized policy family will be $\{\pi_K\}_{K \in \mathcal{S}}$ with $\pi_K(\mathcal{H}_t) := Kx_t$. Lastly, the optimal LQR policy problem becomes

$$\begin{aligned} \min_K \quad & J_{\text{LQR}}(K) \\ \text{subject to} \quad & K \in \mathcal{S}. \end{aligned} \quad (10)$$

For well-posedness of the problem, we assume that the pair (A, B) is stabilizable so \mathcal{S} is non-empty; see Figure 1 for a numerical example.

2.2.2. LQG under Dynamic Output-feedback Policies

We here specify the general closed-loop optimal policy problem (4) in the context of LTI systems with partial observation:

$$x_{t+1} = Ax_t + Bu_t + w_t, \quad y_t = Cx_t + v_t, \quad (11)$$

where $x_t \in \mathbb{R}^n$, $u_t \in \mathbb{R}^m$, $y_t \in \mathbb{R}^p$ are the system state, input, and output measurement at time t , and $w_t \sim \mathcal{N}(0, W)$, $v_t \sim \mathcal{N}(0, V)$ are Gaussian process and measurement noise signals, respectively. It is assumed that the covariance matrices satisfy $W \succeq 0, V \succ 0$. Given performance weight matrices $Q \succeq 0, R \succ 0$, the optimal LQG problem becomes,

$$\min_{\pi \in \Pi} \quad J_{\text{LQG}}(\mathbf{u}) := \lim_{T \rightarrow \infty} \mathbb{E}_{\mathbf{w}, x_0} \frac{1}{T} J_T(\mathbf{u}, \mathbf{w}, x_0) \quad (12a)$$

$$\text{subject to} \quad (11), u_t = \pi(\mathcal{H}_t) \quad (12b)$$

where $\mathbf{w} := ((w_t, v_t))_{t=0}^\infty$. It should be noted that the difference between the optimal closed-loop policy problems (12) and (7) is the policies have to be output-feedback with $\mathcal{H}_t = (u_{0:t-1}, y_{0:t-1})$ versus state-feedback with $\mathcal{H}_t = (u_{0:t-1}, x_{0:t})$, respectively.

Next, we construct a family of policies, referred to as *dynamic policies*, parameterized by an LTI system,

$$\xi_{t+1} = A_K \xi_t + B_K y_t, \quad u_t = C_K \xi_t, \quad (13)$$

where $\xi_t \in \mathbb{R}^q$ is the controller's internal state at time t , and policy parameters $(A_K, B_K, C_K) \in \mathbb{R}^{q \times q} \times \mathbb{R}^{q \times p} \times \mathbb{R}^{m \times q}$ specify the policy parameters. If $q = n$, we refer to (13) as a *full-order* dynamic policy; if $q < n$, it is called a *reduced-order* dynamic policy. In this survey, we will focus on the case $q = n$ since it is known that full-order dynamic policy parameterization is rich enough; i.e. contains a globally optimal solution to the closed-loop optimal policy problem (12) (Zhou et al., 1996). Therefore, combining (13) with (11) leads to the augmented closed-loop system,

$$\begin{bmatrix} x_{t+1} \\ \xi_{t+1} \end{bmatrix} = \begin{bmatrix} A & BC_K \\ B_K C & A_K \end{bmatrix} \begin{bmatrix} x_t \\ \xi_t \end{bmatrix} + \begin{bmatrix} I & 0 \\ 0 & B_K \end{bmatrix} \begin{bmatrix} w_t \\ v_t \end{bmatrix}, \quad \begin{bmatrix} y_t \\ u_t \end{bmatrix} = \begin{bmatrix} C & 0 \\ 0 & C_K \end{bmatrix} \begin{bmatrix} x_t \\ \xi_t \end{bmatrix} + \begin{bmatrix} v_t \\ 0 \end{bmatrix}. \quad (14)$$

The set of stabilizing controllers with order $q \in \mathbb{N}$ is now defined as,

$$\Theta := \mathcal{C}_q = \left\{ K = \begin{bmatrix} 0_{m \times p} & C_K \\ B_K & A_K \end{bmatrix} \in \mathbb{R}^{(m+q) \times (p+q)} \mid \rho \left(\begin{bmatrix} A & BC_K \\ B_K C & A_K \end{bmatrix} \right) < 1 \right\}. \quad (15)$$

Then, any such $K \in \mathcal{C}_q$ determines a dynamic policy π_K with $\pi_K(\mathcal{H}_t) := \sum_{i=1}^t C_K A_K^{i-1} B_K y_{t-i}$, where we set $\xi_0 = 0$. Following the parameterization in (5), given the system plant dimension n , the policy optimization for LQG control becomes

$$\begin{aligned} & \min_K J_{\text{LQG}}(K) \\ & \text{subject to } K \in \mathcal{C}_n. \end{aligned} \quad (16)$$

Throughout this survey, we make the standard assumption that (A, B) is stabilizable and (C, A) is detectable for the LTI system (11), so that \mathcal{C}_n is nonempty.

2.2.3. \mathcal{H}_∞ -robust Control under Static State-feedback Policies

The \mathcal{H}_∞ -norm of a closed-loop transfer function characterizes the worst case performance against adversarial disturbances w_t with bounded energy. Considering the same dynamics in (6), then (4) reduces to the \mathcal{H}_∞ robust control problem:

$$\begin{aligned} & \min_{\pi \in \Pi} J_\infty(\mathbf{u}) := \sup_{\|\mathbf{w}\|_{l_2} \leq 1} \lim_{T \rightarrow \infty} J_T(\mathbf{u}, \mathbf{w}, 0) \\ & \text{subject to } (6), u_t = \pi(\mathcal{H}_t), \end{aligned}$$

where we have assumed $x_0 = 0$ for simplicity. Following (5) and by considering the same parameterization as LQR, we can equivalently express J_∞ instead as a function on the set of static stabilizing policies \mathcal{S} , and thus the \mathcal{H}_∞ -robust policy problem becomes,

$$\begin{aligned} & \min_K J_\infty(K) \\ & \text{subject to } K \in \mathcal{S}. \end{aligned} \quad (17)$$

Note that (17) is the state-feedback \mathcal{H}_∞ control based on dynamics in (6), where the *static linear* policy parameterization results in no loss of optimality (Zhou and Khargonekar, 1988). For the partially observed LTI system (11) where the state x_t is not directly measured, we can consider the general output-feedback \mathcal{H}_∞ control, in which a dynamic policy similar to (13) is required (Zhou et al., 1996).

3. Topology and Geometry of Stabilizing Policies

Given an LTI system (6), represented with $(A, B) \in \mathbb{R}^{n \times n} \times \mathbb{R}^{n \times m}$, the set of static stabilizing state-feedback policies $\mathcal{S} \subseteq \mathbb{R}^{m \times n}$ in (9) has rich topological properties. For example, provided (A, B) is stabilizable, we have $\mathcal{S} \neq \emptyset$ and any element of \mathcal{S} can be identified with pole placement (Åström and Murray, 2021). Using the Jury stability criterion (Jury, 1964) (the discrete-time version of the Routh–Hurwitz stability criterion (Parks, 1962)), we can express \mathcal{S} as a finite system of polynomial inequalities written in terms of the elements of $K \in \mathbb{R}^{m \times n}$. However, this set of polynomial inequalities is complicated and may not directly offer insights on topological properties of \mathcal{S} .

It is known that \mathcal{S} is unbounded when $m \geq 2$, and its topological boundary $\partial\mathcal{S} = \{K \in \mathbb{R}^{m \times n} \mid \rho(A + BK) = 1\}$ is a subset of $\mathbb{R}^{m \times n}$. Furthermore, as a result of the continuity of eigenvalues in the entries of the matrix, we can argue that \mathcal{S} is an open set in $\mathbb{R}^{m \times n}$. It can furthermore be shown that \mathcal{S} is contractible. In particular, by the Lyapunov stability linear matrix inequality criterion and a Schur complement argument we can argue that:

Fact 3.1. The set of stabilizing static state-feedback policies \mathcal{S} is path-connected.

This property is vital for devising algorithmic iterates that have to reach a minimizer from any initial point in \mathcal{S} .

3.1. Riemannian Geometry of Stabilizing Policies

Before diving into the geometry of stabilizing policies, we will first introduce basic concepts from Riemannian geometry. More specialized topics will be introduced in their respective sections in this paper. The starting point of departure for us is the realization that the set of stabilizing policies \mathcal{S} , as an open subset of $\mathbb{R}^{m \times n}$, is a smooth manifold; a geometric object, generically denoted by \mathcal{M} , that loosely speaking is locally Euclidean. We call any smooth function $c : \mathbb{R} \rightarrow \mathcal{M}$ a smooth curve on \mathcal{M} . A tangent vector at $x \in \mathcal{M}$ is any vector $\dot{c}(0) = \frac{d}{dt}c(t)|_{t=0}$, where $c(\cdot)$ is a smooth curve passing through x at $t = 0$. The set of all such tangent vectors at x is a vector space called the tangent space at x denoted by $T_x\mathcal{M}$. Its dimension $\dim(T_x\mathcal{M})$ coincides with the dimension of the manifold. For open sets, such as \mathcal{S} , its tangent spaces identifies with the vector space it lies within: $T_K\mathcal{S} \equiv \mathbb{R}^{m \times n}$; this is referred to as the usual identification of the tangent space. The tangent bundle is simply the disjoint union of all tangent spaces $T\mathcal{M} := \{(x, v) : x \in \mathcal{M}, v \in T_x\mathcal{M}\}$.

Let $F : \mathcal{M} \rightarrow \mathcal{N} \subset \mathbb{R}^M$ be a smooth function between two smooth manifolds. If we perturb $x \in \mathcal{M}$ along a direction $v \in T_x\mathcal{M}$, then the perturbation of the output from $F(\cdot)$ is another tangent vector in $T_{F(x)}\mathcal{N}$; the linear mapping $dF_x : T_x\mathcal{M} \rightarrow T_{F(x)}\mathcal{N}$ is called the differential of F at x and acts on any vector $v \in T_x\mathcal{M}$ as

$$dF_x(v) := \left. \frac{d}{dt} \right|_{t=0} (F \circ c)(t)$$

where $c(\cdot)$ is any smooth curve passing x at $t = 0$ with velocity v .

Considering the open set, and hence smooth manifold, of Schur stable matrices \mathcal{A} , we define the Lyapunov mapping $\mathbb{L} : \mathcal{A} \times \mathbb{R}^{n \times n} \rightarrow \mathbb{R}^{n \times n}$ that sends the pair (A, Q) to the unique solution P of

$$P = APA^\top + Q. \tag{18}$$

The following lemma is instrumental in geometric analysis of policies for linear systems.

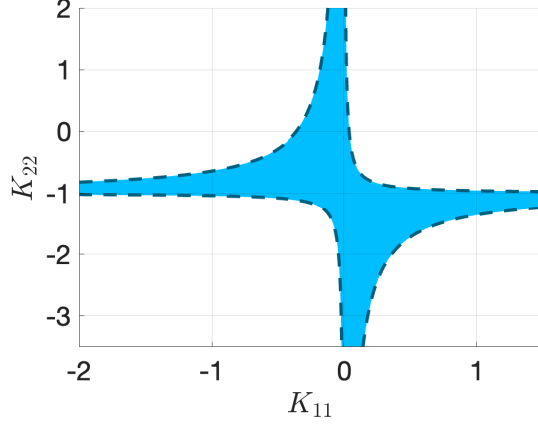


Figure 2: The 2-dimensional set of stabilizing policies subject to the off-diagonal sparsity constraint. The LTI system is $A = \begin{bmatrix} 0.8 & 1 \\ 0 & 0.8 \end{bmatrix}$ and $B = \begin{bmatrix} 0 & 1 \\ 1 & 0 \end{bmatrix}$.

Lemma 3.1. *The differential of \mathbb{L} at $(A, Q) \in \mathcal{A} \times \mathbb{R}^{n \times n}$ along $(E, F) \in T_{(A, Q)}(\mathcal{A} \times \mathbb{R}^{n \times n}) \cong \mathbb{R}^{n \times n} \times \mathbb{R}^{n \times n}$ is*

$$d \mathbb{L}_{(A, Q)}[E, F] = \mathbb{L}(A, E \mathbb{L}(A, Q) A^\top + A \mathbb{L}(A, Q) E^\top + F).$$

For any $A \in \mathcal{A}$ and $Q, \Sigma \in \mathbb{R}^{n \times n}$ we further have the so-called Lyapunov-trace property,

$$\text{tr} [\mathbb{L}(A^\top, Q) \Sigma] = \text{tr} [\mathbb{L}(A, \Sigma) Q].$$

Moving on, a Riemannian metric $\langle \cdot, \cdot \rangle_x : T_x \mathcal{M} \times T_x \mathcal{M} \rightarrow \mathbb{R}$ on a smooth manifold \mathcal{M} is an inner product that smoothly varies in x with $x \in \mathcal{M}$. We call $(\mathcal{M}, \langle \cdot, \cdot \rangle)$ a Riemannian manifold and often add a superscript to clarify specific Riemannian metrics. A (locally-defined) retraction is a smooth mapping $\mathcal{R} : \mathcal{T} \subset T\mathcal{M} \rightarrow \mathcal{M}$ where \mathcal{T} contains an open subset of $(x, 0_x) \in \mathcal{T}$ for each $x \in \mathcal{M}$, and the curve $c(t) := \mathcal{R}(x, tv)$ satisfies $c(0) = x$ and $\dot{c}(0) = v$.

The upshot of introducing Riemannian geometry for policy optimization is now as follows. For any static feedback policy $K \in \mathcal{S}$, define the following Riemannian metric that depends on a solution of a Lyapunov equation³:

$$\langle V, W \rangle_K^{\mathbb{L}} := \text{tr} [V^\top W Y_K],$$

where $Y_K := \mathbb{L}(A + BK, \Sigma)$. In fact, this dependence varies smoothly in policy K and thus we can show that $\langle \cdot, \cdot \rangle^{\mathbb{L}}$ is a Riemannian metric on \mathcal{S} referred to as the ‘‘Lyapunov metric.’’

Theorem 3.2. *If $\Sigma \succ 0$ then $(\mathcal{S}, \langle \cdot, \cdot \rangle^{\mathbb{L}})$ is a Riemannian manifold.*

The Riemannian machinery introduced for stabilizing policies also allows addressing feedback design for certain classes of *constrained* policies. For example, when $\mathcal{K} \subset \mathbb{R}^{m \times n}$ and we restrict the policies to $\Theta = \tilde{\mathcal{S}} := \mathcal{S} \cap \mathcal{K}$. From a *topological* perspective, $\tilde{\mathcal{S}} \subset \mathcal{S}$ remains relatively open as \mathcal{S} was open in $\mathbb{R}^{m \times n}$. However, in general, $\tilde{\mathcal{S}}$ is not only non-convex (Ackermann, 1980) but also disconnected (Feng and Lavaei, 2019). Nonetheless, one can show that sparsity constraint

³Compare with the Frobenius inner product $\langle V, W \rangle^{\text{F}} = \text{tr} [V^\top W]$ which induces the so-called Euclidean geometry.

(which is of primary interest in network systems) and static output feedback policies lead to properly embedded submanifolds of \mathcal{S} (Talebi and Mesbahi, 2022), thus entailing this Riemannian geometry as summarized in the following. See Figure 2 for a numerical example of $\tilde{\mathcal{S}}$ with a sparsity constraint.

Fact 3.2. For any sparsity constraint $\mathcal{K}_D := \{K \in \mathbb{R}^{m \times n} \mid K_{i,j} = 0, (i,j) \notin D\}$ with a index set $D \subset [m] \times [n]$, the set of sparse stabilizing policies $\tilde{\mathcal{S}} = \mathcal{S} \cap \mathcal{K}_D \subset \mathcal{S}$ is a properly embedded submanifold of dimension $|D|$. Also, each tangent space at $K \in \tilde{\mathcal{S}}$ identifies with $T_K \tilde{\mathcal{S}} \cong \mathcal{K}_D$.

Fact 3.3. For any output feedback constraint $\mathcal{K}_C := \{K \in \mathbb{R}^{m \times n} \mid K = LC, L \in \mathbb{R}^{m \times d}\}$ with a full-rank output matrix C , the set of static output-feedback policies $\tilde{\mathcal{S}} = \mathcal{S} \cap \mathcal{K}_C$ is a properly embedded submanifold of \mathcal{S} with dimension md . Also, each tangent space at $K \in \tilde{\mathcal{S}}$ identifies with $T_K \tilde{\mathcal{S}} \cong \mathcal{K}_C$.

We later see the implications of these fact when we study the (Riemannian) gradient and Hessian of a smooth cost in §4.3.2.

3.2. Topology and Geometry of Dynamic Output-feedback Polices

Herein, we focus on the output-feedback problem setup introduced in §2.2.2. Our parameterized family of policies will be the set of full-order dynamic output feedback policies $\Theta := \mathcal{C}_n$ in (15), and we next discuss some of its topological and geometrical properties.

Similar to the static case, \mathcal{C}_n is a nonconvex set. This is illustrated in Figure 3 with a numerical example. It is also known that the set \mathcal{C}_n is open and unbounded. In addition to the non-convexity, the set \mathcal{C}_n can even be disconnected but has at most two diffeomorphic components that are captured by the following notion of “similarity transformations in control”: for any invertible matrix $T \in \text{GL}_n$, define the mapping \mathcal{T}_T that sends any dynamic policy \mathbf{K} to

$$\mathcal{T}_T(\mathbf{K}) := \begin{bmatrix} 0 & C_{\mathbf{K}} T^{-1} \\ T B_{\mathbf{K}} & T A_{\mathbf{K}} T^{-1} \end{bmatrix}. \quad (19)$$

Note that the policy $\mathbf{K} \in \mathcal{C}_n$ if and only if the transformed policy $\mathcal{T}_T(\mathbf{K}) \in \mathcal{C}_n$. Indeed, the map $\mathbf{K} \mapsto \mathcal{T}_T(\mathbf{K})$ is a diffeomorphism from \mathcal{C}_n to itself for any such invertible matrix T .⁴

Fact 3.4. The set \mathcal{C}_n has at most two path-connected components. If \mathcal{C}_n has two path-connected components $\mathcal{C}_n^{(1)}$ and $\mathcal{C}_n^{(2)}$, then $\mathcal{C}_n^{(1)}$ and $\mathcal{C}_n^{(2)}$ are diffeomorphic under the mapping \mathcal{T}_T , for any invertible matrix $T \in \mathbb{R}^{n \times n}$ with $\det T < 0$.

The potential disconnectivity of \mathcal{C}_n comes from the fact that the set of real invertible matrices $\text{GL}_n = \{\Pi \in \mathbb{R}^{n \times n} \mid \det \Pi \neq 0\}$ has two path-connected components: $\text{GL}_n^+ = \{\Pi \in \mathbb{R}^{n \times n} \mid \det \Pi > 0\}$, $\text{GL}_n^- = \{\Pi \in \mathbb{R}^{n \times n} \mid \det \Pi < 0\}$. In other words, the nature of similarity transformations embedded in dynamic feedback policies may cause \mathcal{C}_n to be disconnected. The following results provide conditions that ensure \mathcal{C}_n to be a single path-connected component.

Fact 3.5. If there exists a reduced-order stabilizing policy for (11), i.e., $\mathcal{C}_{n-1} \neq \emptyset$, then \mathcal{C}_n is path-connected. The converse also holds for systems with single-input or single-output, i.e., when $m = 1$ or $p = 1$ in (11).

⁴Note that the same input-output behavior of a policy (13) can be represented using different state-space models, e.g., using different coordinates for the internal policy state which is precisely captured by this similarity transformation.

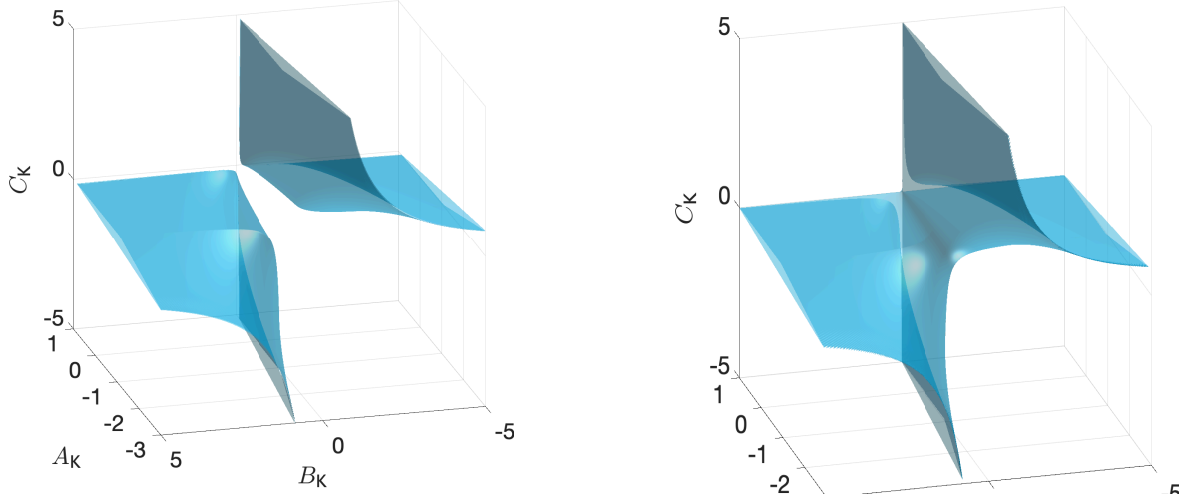


Figure 3: Illustration of the set of dynamic stabilizing policies \mathcal{C}_1 for an LTI system with $B = C = 1$ and: (a) with $A = 1.1$ resulting in two path-connected components; (b) with $A = 0.9$ resulting in a single path-connected component.

We can immediately deduce the following facts: 1) For any open-loop unstable first-order dynamical system, *i.e.*, $n = 1$ and $A > 0$, there exist no reduced-order stabilizing policies, *i.e.*, $\mathcal{C}_{n-1} = \emptyset$; thus its associated set of stabilizing policies \mathcal{C}_n must be disconnected. 2) For any open-loop stable systems, *i.e.*, when A is stable, we naturally have a reduced-order stabilizing policy, and thus the corresponding set of stabilizing policies is always path-connected. Figure 3 provides numerical examples for each case.

3.3. Symmetries of Dynamic Output-feedback Policies: a Quotient Geometry

An alternative parameterization for dynamic output-feedback systems (15) is through turning \mathcal{C}_n into a Riemannian quotient manifold of lower dimension. To see this, note that the group of similarity transformations $\{\mathcal{T}_T(\cdot) : T \in \text{GL}_n\} \equiv \text{GL}_n$ is a group action acting smoothly on \mathcal{C}_n . Recall, we are treating the open subset $\mathcal{C}_n \subset \mathbb{R}^{(n+m) \times (n+p)}$ as a smooth manifold. The orbit of $\mathbf{K} \in \mathcal{C}_n$ is then the collection of controllers reachable from \mathbf{K} via similarity transformation:

$$[\mathbf{K}] := \left\{ \begin{bmatrix} 0 & C_{\mathbf{K}}T^{-1} \\ TB_{\mathbf{K}} & TA_{\mathbf{K}}T^{-1} \end{bmatrix} : T \in \text{GL}_n \right\}.$$

A few examples of such orbits are shown in Figure 4 in distinct colors. Recall that LQG cost is constant on each orbit; this serves as the basis for the PO for LQG over the so-called quotient space.

The quotient set (also known as the orbit set) of \mathcal{C}_n is simply the collection of all orbits:

$$\mathcal{C}_n/\text{GL}_n := \{[\mathbf{K}] : \mathbf{K} \in \mathcal{C}_n\}.$$

We equip $\mathcal{C}_n/\text{GL}_n$ with the induced quotient topology, defined as the finest topology in which the quotient map $\pi : \mathcal{C}_n \rightarrow \mathcal{C}_n/\text{GL}_n$, sending each \mathbf{K} to the orbit $[\mathbf{K}]$, is continuous. The resulting topological space is called the quotient space.

The next step is to design a smooth structure for $\mathcal{C}_n/\text{GL}_n$, turning it into a smooth manifold. For arbitrary quotient spaces, if there exists a smooth structure in which the quotient map is a smooth submersion, we call the resulting quotient space a smooth quotient manifold. In this

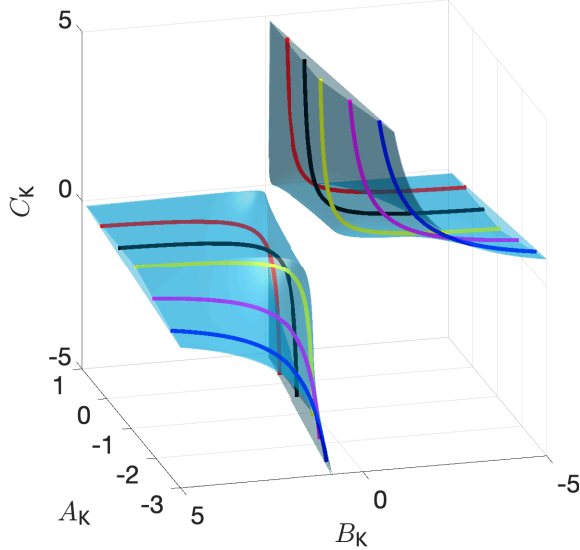


Figure 4: The region of stabilizing dynamic feedback policies $\mathcal{C}_1 \subset \mathbb{R}^3$ for the plant $(A, B, C) = (1.1, 1, 1)$. Each colored curve (red, purple, yellow, magenta, dark blue) is an individual orbit of policies. Note that \mathcal{C}_1 has 2 path-connected components.

context, the original smooth manifold is called the total manifold. Unfortunately, quotient spaces are often not even Hausdorff. Recall a topological space is Hausdorff when any pair of points can be separated into disjoint neighborhoods of the corresponding points; this property implies all sequences have a unique limit. Therefore for non-Hausdorff quotient spaces, optimization is hopeless because limits cannot even be defined!

As it turns out, $\mathcal{C}_n/\text{GL}_n$ is non-Hausdorff. The reason is the existence of non-controllable and non-observable, yet stabilizing, dynamic controllers which acts as “jumps.” This is explained in more detail in Hazewinkel (1976). Fortunately, the quotient space $\mathcal{C}_n^{\min}/\text{GL}_n$ is Hausdorff (Kraisler and Mesbahi, 2024, Lemma 4.1), where \mathcal{C}_n^{\min} are all full-order *minimal* policies—policies with controllable and observable state space form. This follows from the remarkable theorem in Hazewinkel (1976) proving the orbit space of minimal linear systems admits a smooth quotient manifold structure. It can be shown $\dim(\mathcal{C}_n^{\min}/\text{GL}_n) = nm + np$, an order of magnitude smaller. So, in the context of smooth optimization, we have a significantly smaller search space.

Before we continue, let us discuss the tangent space of \mathcal{C}_n . As an open subset, the tangent space of \mathcal{C}_n coincides with its linear span: tangent *vectors* to the open set \mathcal{C}_n are simply

$$\mathbf{V} = \begin{bmatrix} 0 & G \\ F & E \end{bmatrix}$$

for any matrices $E \in \mathbb{R}^{n \times n}$, $F \in \mathbb{R}^{n \times p}$, and $G \in \mathbb{R}^{m \times n}$. The resulting vector space will be denoted \mathcal{V}_n ; so, we write $T_K \mathcal{C}_n \equiv \mathcal{V}_n$.

In order to adopt smooth optimization techniques for $\mathcal{C}_n^{\min}/\text{GL}_n$, we at last must equip the smooth quotient manifold with a retraction and Riemannian metric. To do this, we will discuss a correspondence of these two constructs between the total manifold \mathcal{C}_n^{\min} and the quotient manifold $\mathcal{C}_n^{\min}/\text{GL}_n$. We can show that there is an invertible correspondence between Riemannian metrics on $\mathcal{C}_n^{\min}/\text{GL}_n$ and *similarity-invariant* Riemannian metrics on \mathcal{C}_n^{\min} , by which we mean

$$\langle \mathbf{V}, \mathbf{W} \rangle_K = \langle \mathcal{I}_T(\mathbf{V}), \mathcal{I}_T(\mathbf{W}) \rangle_{\mathcal{I}_T(K)}. \quad (20)$$

A related correspondence holds for retractions. See (Boumal, 2023, §9) and (Kraisler and Mesbahi, 2024, §4) for how to induce such a Riemannian metric and retraction onto the quotient manifold.

Now we will define a similarity-invariant Riemannian metric satisfying (20). Let $A_{\text{cl}}(\mathbf{K}), B_{\text{cl}}(\mathbf{K})$, and $C_{\text{cl}}(\mathbf{K})$ denote the matrices corresponding to the (augmented) closed-loop system in (14). A consequence of the minimality of any $\mathbf{K} \in \mathcal{C}_n^{\text{min}}$ is (1) $A_{\text{cl}}(\mathbf{K})$ is Hurwitz and (2) the closed loop system $(A_{\text{cl}}(\mathbf{K}), B_{\text{cl}}(\mathbf{K}), C_{\text{cl}}(\mathbf{K}))$ is also minimal. The latter follows from the Popov-Belevitch-Hautus test. As a result, the controllability and observability Grammians of the closed-loop system satisfy

$$\mathcal{W}_c(\mathbf{K}) := \mathbb{L}(A_{\text{cl}}(\mathbf{K}), B_{\text{cl}}(\mathbf{K})B_{\text{cl}}(\mathbf{K})^\top) > 0 \quad (21a)$$

$$\mathcal{W}_o(\mathbf{K}) := \mathbb{L}(A_{\text{cl}}(\mathbf{K}), C_{\text{cl}}(\mathbf{K})^\top C_{\text{cl}}(\mathbf{K})) > 0. \quad (21b)$$

Now, we introduced the so-called ‘‘Krishnaprasad-Martin (KM) metric’’ defined as

$$\langle \mathbf{V}_1, \mathbf{V}_2 \rangle_{\mathbf{K}}^{\text{KM}} := w_1 \text{tr}[\mathcal{W}_o(\mathbf{K}) \cdot \mathbf{E}(\mathbf{V}_1) \cdot \mathcal{W}_c(\mathbf{K}) \cdot \mathbf{E}(\mathbf{V}_2)^\top] \quad (22a)$$

$$+ w_2 \text{tr}[\mathbf{F}(\mathbf{V}_1)^\top \cdot \mathcal{W}_o(\mathbf{K}) \cdot \mathbf{F}(\mathbf{V}_2)] \quad (22b)$$

$$+ w_3 \text{tr}[\mathbf{G}(\mathbf{V}_1) \cdot \mathcal{W}_c(\mathbf{K}) \cdot \mathbf{F}(\mathbf{V}_2)^\top] \quad (22c)$$

where $w_1 > 0$ and $w_2, w_3 \geq 0$ are design constants and

$$\mathbf{E}(\mathbf{V}) := \begin{bmatrix} 0 & BG \\ FC & E \end{bmatrix}, \quad \mathbf{F}(\mathbf{V}) := \begin{bmatrix} 0 & 0 \\ 0 & F \end{bmatrix}, \quad \mathbf{G}(\mathbf{V}) := \begin{bmatrix} 0 & 0 \\ 0 & G \end{bmatrix}.$$

We can show that the inner-product in (22) varies smoothly in \mathbf{K} and, by referring to (21a) for each $\mathbf{K} \in \mathcal{C}_n^{\text{min}}$, establish the following result (analogous to the Riemannian metric in Theorem 3.2).

Theorem 3.3. *The mapping that sends each $\mathbf{K} \in \mathcal{C}_n^{\text{min}}$ to the inner-product $\langle \cdot, \cdot \rangle_{\mathbf{K}}^{\text{KM}}$ induces a Riemannian metric on $\mathcal{C}_n^{\text{min}}$ which is similarity-invariant; i.e., satisfies (20).*

4. Geometry of Performance Objectives on Stabilizing Policies

In this section, we turn our attention toward performances measures described in §2 and the interplay of domain geometry and the landscape of the cost functions associated with each performance measure. Before getting to each specific metric, we review some of the geometric constructs that are essential in characterizing the first and second-order variations of smooth cost functions, subsequently used for optimization.

4.1. Riemannian Geometry and Policy Optimization

For brevity, we introduce these constructs for the smooth manifold \mathcal{S} which also holds for any other smooth manifold. A vector field $V : \mathcal{S} \rightarrow T\mathcal{S}$ is a mapping that smoothly assigns every $K \in \mathcal{S}$ to a tangent vector $V_K \in T_K\mathcal{S}$. A vector field induces a mapping on the space of smooth functions, sending $J : \mathcal{S} \rightarrow \mathbb{R}$ to $VJ : \mathcal{S} \rightarrow \mathbb{R}$ as follows:

$$VJ(K) := dJ_K(V_K) \quad (23)$$

In this section, to distinguish tangent vectors from vector fields, we will denote the former with V_K to emphasize that V_K is a tangent vector in $T_K\mathcal{S}$. Now, we can define the (Riemannian)

gradient of J with respect to the Riemannian metric $\langle \cdot, \cdot \rangle^L$ on \mathcal{S} , denoted by $\text{grad } J$. In particular, $\text{grad } J$ is the unique vector field satisfying

$$\langle V, \text{grad } J \rangle^L = VJ, \quad (24)$$

for all vector fields V .

In order to define second-order variations of a smooth functions J , such as the Riemannian Hessian, we must introduce a notion of directional derivatives on manifolds. This is referred to as the *(affine) connection*, denoted by ∇ . Consider two vector fields V and W on \mathcal{S} . Then, the connection ∇ allows us to define $\nabla_V W$, which itself is a vector field, at each $K \in \mathcal{S}$ as the directional derivative of W along $V_K \in T_K \mathcal{S}$. Each Connection on \mathcal{S} is uniquely identified with $\dim(\mathcal{S})^3$ number of smooth functions on \mathcal{S} called the *Christoffel Symbols*. With the Christoffel Symbols associated with ∇ , in order to compute $(\nabla_V W)_K$, we only need the direction V_K and the vector field W locally; we do not need other evaluations of V .

Every Riemannian metric uniquely induces a *compatible* affine connection known as the *Levi-Civita connection*. It is the unique connection which satisfies

$$\nabla_U \langle V, W \rangle = \langle \nabla_U V, W \rangle + \langle V, \nabla_U W \rangle \quad (25)$$

for any vector fields U, V, W of \mathcal{S} .⁵ Hereafter, we let ∇ and $\bar{\nabla}$ denote the Levi-Civita connections of \mathcal{S} compatible with $\langle \cdot, \cdot \rangle^L$ and the Frobenius inner product $\langle V, W \rangle^F := \text{tr} [V^T W]$, respectively. The macron in $\bar{\nabla}$ indicates the “flatness” of this Euclidean directional derivative.

Letting $\mathfrak{X}(\mathcal{S})$ denote the family of vector fields on \mathcal{S} , we can define the Riemannian Hessian of J in two equivalent ways:

$$\text{Hess } J(V) := \nabla_V \text{grad } J \quad (26a)$$

$$\text{Hess } J(V, W) := \langle \nabla_V \text{grad } J, W \rangle^L \quad (26b)$$

for any $V, W \in \mathfrak{X}(\mathcal{S})$. Both forms can be used interchangeably. The former is used in the context of Riemannian-Newton optimization. The latter is used in the context of defining a matrix representing the Hessian matrix of f . It should be noted that for both definitions, V and W do not have to be tangent vector *fields*; they could simply be tangent vectors. To emphasize our evaluation at a specific $K \in \mathcal{S}$, we will write $\text{Hess } J|_K$ for both definitions.

As usual, the Euclidean Hessian is equivalently defined as $\bar{\nabla}^2 J(V) := \bar{\nabla}_V \bar{\nabla} J$. At last, we also introduce an atypical yet efficient notion known as the pseudo-Euclidean Hessian which essentially ignores the curvature of the manifold in quantifying the second order behavior of a smooth function. It is constructed by applying the *Euclidean affine connection* $\bar{\nabla}$ on the (Riemannian) gradient $\text{grad } J$ as follows:

$$\bar{\text{Hess}} J(V) := \bar{\nabla}_V \text{grad } J \quad (27)$$

which will be compared with the Riemannian Hessian, denoted by $\text{Hess } J$.

⁵To be precise, for technical reasons regarding the uniqueness we must also require that ∇ is “symmetric;” see [Talebi and Mesbahi \(2023\)](#).

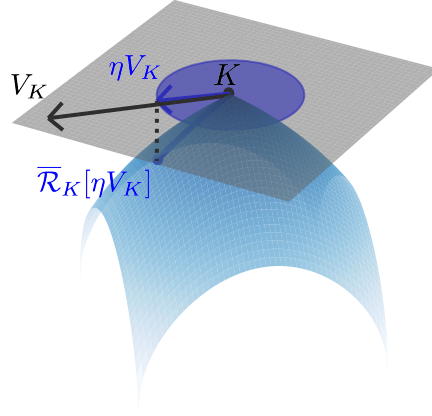


Figure 5: Local retraction defined by the stability certificate: A schematic of the gray plane exemplifying a tangent space at a point K on the blue manifold. The stability certificate provides a (purple) neighborhood of the origin (in every tangent space) such that an efficient “local retraction” $\bar{\mathcal{R}}_K$ can be obtained, such that every tangent vector V_K can be “retracted” to $\bar{\mathcal{R}}_K[\eta V_K]$ after proper scaling by the stability certificate s_K with $\eta := s_K(V_K)$.

4.2. Stability Certificate for the Euclidean Retraction

For the open submanifold of a vector space, such as the static feedback policies \mathcal{S} , a useful example of a retraction is the Euclidean retraction: $\bar{\mathcal{R}}_K(V_K) := K + V_K$, which is computationally efficient. We emphasize that this is not well-defined globally on $T_K\mathcal{S}$, and thus motivates us to further determine the local neighborhood on which it will be well-defined; see Figure 5.

Lemma 4.1. *For any direction $V_K \in T_K\mathcal{S} \cong \mathbb{R}^{m \times n}$ at any point $K \in \mathcal{S}$, if*

$$0 \leq \eta \leq s_K(V_K) := \frac{1}{2\lambda_{\max}(\mathbb{L}(A_{cl}^\top, I)) \|BV_K\|_2}$$

where $A_{cl} = A + BK$, then $\bar{\mathcal{R}}_K(\eta V_K) = K + \eta V_K \in \mathcal{S}$.

A few remarks are in order. First, since $\mathcal{S} \subset \mathbb{R}^{m \times n}$ is open, the stability certificate offers a closed-form expression of a continuous lower bound on the radius to instability: $s_K(V_K) \leq \sup\{t : t > 0, K + tV_K \in \mathcal{S}\}$, which has an unknown closed-form expression. In the structured LQR setup, since \mathcal{K} is an affine space, $\tilde{\mathcal{S}}$ is relatively open and thus $s_K(\cdot)$ is also a stability certificate on $\tilde{\mathcal{S}}$. Given $K \in \tilde{\mathcal{S}}$ and $V_K \in T_K\tilde{\mathcal{S}}$, then

$$K^+ := \bar{\mathcal{R}}_K(\eta V_K) = K + \eta V_K \tag{28}$$

for $\eta = \min(1, s_K(V_K))$ renders $K^+ \in \tilde{\mathcal{S}}$. Thus, for iterative update of policy K in (28), the chosen step size guarantees feasibility and stability of $K^+ \in \tilde{\mathcal{S}}$.

For the LQR setup, the direction V_K could be the negated Riemannian gradient $-\text{grad } J_{\text{LQR}}(K)$ or Euclidean gradient $-\bar{\nabla} J_{\text{LQR}}(K)$ of the LQR cost. The direction could also incorporate second-order information, in the form of a Riemannian-Newton optimization, formulated as the solution $V_K \in T_K\mathcal{S}$ of any of these linear equations:

$$\begin{aligned} \text{Hess } J_{\text{LQR}}|_K(V) &= -\text{grad } J_{\text{LQR}}(K) \\ \bar{\nabla}^2 J_{\text{LQR}}|_K(V) &= -\bar{\nabla} J_{\text{LQR}}(K) \\ \overline{\text{Hess}} J_{\text{LQR}}|_K(V) &= -\text{grad } J_{\text{LQR}}(K). \end{aligned}$$

Additionally, for structured LQR setup, we show that these first and second order variations can be obtained similarly for the constrained cost $\tilde{J} = J|_{\tilde{\mathcal{S}}}$ using [Theorem 4.4](#) and the policy update proceeds similarly.

Remark 1. In the absence of constraint when $\tilde{\mathcal{S}} = \mathcal{S}$, the Hwer’s algorithm introduces the following updates $K^+ = -(R + B^\top P_K B)^{-1} B^\top P_K A$ with $P_K = \mathbb{L}(A_{\text{cl}}^\top, Q + K^\top R K)$, which is shown to converge to the global optimum quadratically. Somewhat interestingly, it in can be written as $K^+ = K + \hat{V}$, with a “Riemannian quasi-Newton” direction \hat{V}_t satisfying,

$$\hat{H}_K \hat{V} = -\text{grad } J_{\text{LQR}}(K),$$

where $\hat{H}_K := R + B^\top P_K B$ is a positive definite approximation of $\text{Hess } J_{\text{LQR}}|_K$ and $\overline{\text{Hess}} J_{\text{LQR}}|_K$. The *algebraic coincidence* is that the unit stepsize remains stabilizing throughout these quasi-Newton updates. We will also see that for the unconstrained LQR problem a small enough (fixed) step-size is sufficient. In general though, we do not expect such step sizes to be stabilizing, and particularly on constrained submanifolds $\tilde{\mathcal{S}}$ one needs to instead utilize the stability certificate developed in [Lemma 4.1](#) to guarantee the stability of each policy iterate.

4.3. Linear Quadratic Regulator (LQR)

We here discuss the non-convex geometry in the policy optimization for LQR. We consider both the standard (unconstrained) case, where the policy parameter K can be a dense matrix, and the constrained case, where K has extra linear constraints in addition to the stabilizing requirement—such as sparsity or output measurement.

4.3.1. Unconstrained Case

First, by the Lyapunov-trace property in [Lemma 3.1](#), one can show that for the static feedback parameterization $u_t = K x_t$ where $K \in \mathcal{S}$, both the cost functions in (7) and (8) are equivalent with

$$J_{\text{LQR}}(K) = \frac{1}{2} \text{tr} [P_K \Sigma] = \frac{1}{2} \text{tr} [(Q + K^\top R K) Y_K], \quad (29)$$

where $P_K = \mathbb{L}(A_{\text{cl}}^\top, Q + K^\top R K)$, $Y_K = \mathbb{L}(A_{\text{cl}}, \Sigma)$, and $A_{\text{cl}} = A + BK$. Next, the first and second variations of the smooth cost $J_{\text{LQR}} \in C^\infty(\mathcal{S})$ with respect to the Riemannian and Euclidean metrics are obtained in the following proposition.

Proposition 4.2. *Consider the Riemannian manifold $(\mathcal{S}, \langle \cdot, \cdot \rangle^{\text{L}})$. Then $J_{\text{LQR}}(\cdot)$ is smooth and*

$$\begin{aligned} \text{grad } J_{\text{LQR}}(K) &= RK + B^\top P_K A_{\text{cl}} \\ \overline{\nabla} J_{\text{LQR}}(K) &= (RK + B^\top P_K A_{\text{cl}}) Y_K. \end{aligned}$$

See [Talebi and Mesbahi \(2023\)](#) for explicit formulae of the Riemannian Hessian, and other second order variations of J_{LQR} .

Next, we review the properties of this cost function critical to policy optimization.

Lemma 4.3. *Suppose $\Sigma, Q, R \succ 0$ and (A, B) is stabilizable. Then, the function $J_{\text{LQR}}(\cdot): \mathcal{S} \rightarrow \mathbb{R}$,*

(a) *is real analytic, and in particular smooth.*

(b) *is coercive: $K \rightarrow \partial\mathcal{S}$ or $\|K\|_F \rightarrow \infty$ implies $J_{\text{LQR}}(K) \rightarrow \infty$;*

(c) admits a unique global minimum K^* on \mathcal{S} satisfying $K^* = -(R + B^\top P_K B)^{-1} B^\top P_K A$;

(d) has compact sublevel sets $\mathcal{S}_\alpha := \{K : J_{\text{LQR}}(K) \leq \alpha\}$ for each finite α ;

(e) is gradient dominant on each sublevel set: there exists a constant $c_1 > 0$ such that

$$c_1 [J_{\text{LQR}}(K) - J_{\text{LQR}}(K^*)] \leq \|\bar{\nabla} J_{\text{LQR}}(K)\|_F^2, \quad \forall K \in \mathcal{S}_\alpha;$$

(f) has L -Lipchitz gradient on each sublevel set: there exists a constant $L > 0$ such that

$$\|\bar{\nabla} J_{\text{LQR}}(K) - \bar{\nabla} J_{\text{LQR}}(K')\|_F \leq L \|K - K'\|_F, \quad \forall K, K' \in \mathcal{S}_\alpha;$$

(g) admits lower and upper quadratic models on each sublevel set: there exists constants $c_2 > 0$ and $c_3 > 0$ such that

$$c_2 \|K - K^*\|_F^2 \leq J_{\text{LQR}}(K) - J_{\text{LQR}}(K^*) \leq c_3 \|K - K^*\|_F^2, \quad \forall K \in \mathcal{S}_\alpha.$$

These properties of J_{LQR} are quite essential in providing theoretical guarantees for different optimization schemes. In particular, the smoothness, Lipschitz continuity, and quadratic models are common in convex optimization whereas the gradient dominance enables global convergence guarantees despite non-convexity of J_{LQR} in K . Finally, note that these properties holds on each (fixed) sublevel set of the cost which often is chosen to contain the initial policy K_0 . These has been made possible due to the coercive property of J_{LQR} that results in compact sublevel sets.

4.3.2. Linearly Constrained Case

Here, we will discuss the Riemannian geometry of the LQR cost in the structured LQR setup. Since $\tilde{\mathcal{S}} := \mathcal{S} \cap \mathcal{K} \subset \mathcal{S}$ is an embedded submanifold, the Riemannian metric $\langle \cdot, \cdot \rangle^{\text{L}}$ can be equipped onto $\tilde{\mathcal{S}}$ simply by restricting its domain $T\mathcal{S}$ onto $T\tilde{\mathcal{S}}$. Also, for any smooth function J on \mathcal{S} , we let $\tilde{J} := J|_{\tilde{\mathcal{S}}}$ be its restriction to $\tilde{\mathcal{S}}$. However, the gradient and Hessian of \tilde{J} will not relate to those of J so simply. As for gradient $\text{grad } \tilde{J} : \tilde{\mathcal{S}} \rightarrow T\tilde{\mathcal{S}}$, our Euclidean intuition is correct and so it can be related to $\text{grad } J$ by the ‘‘tangential projection’’ operator π^\top —the generalization of orthogonal projection with respect to the Riemannian metric. On the other hand, for the Riemannian Hessian of this restricted cost, denoted by $\text{Hess } \tilde{J}$, our Euclidean intuition fails as this correspondence cannot be explained by merely a projection operator. In fact, the curvature of the underlying Riemannian manifold affects this second-order information. This can be captured precisely by the *Weingarten map* $\mathbb{W}_U(V) \in \mathfrak{X}(\tilde{\mathcal{S}})$ as the unique vector field satisfying

$$\langle \mathbb{W}_U(V), W \rangle^{\text{L}} = \langle U, \nabla_V W - \pi^\top \nabla_V W \rangle^{\text{L}} \quad (30)$$

for all $W \in \mathfrak{X}(\tilde{\mathcal{S}})$. These relations are summarized below; see [Talebi and Mesbahi \(2023\)](#) for further details.

Theorem 4.4. *Let $J : \mathcal{S} \rightarrow \mathbb{R}$ and $\tilde{J} := J|_{\tilde{\mathcal{S}}}$. Then over $\tilde{\mathcal{S}}$, we have*

$$\text{grad } \tilde{J} = \pi^\top \text{grad } J. \quad (31)$$

Furthermore, for any $V \in \mathfrak{X}(\tilde{\mathcal{S}})$, we have

$$\text{Hess } \tilde{J}(V) = \pi^\top \text{Hess } J(V) + \mathbb{W}_U(V), \quad (32)$$

where $U := \text{grad } J - \pi^\top \text{grad } J$.

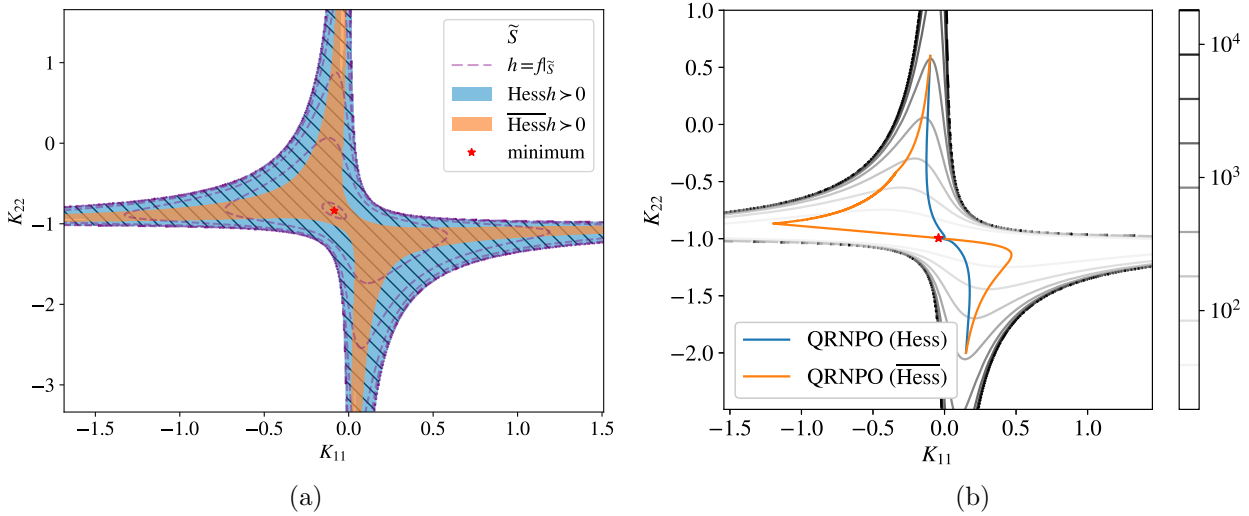


Figure 6: A numerical example for the feasible set of diagonal stabilizing controller for the SLQR problem of §2. a) the region on which the Riemannian Hessian is positive definite versus that of Pseudo-Euclidean Hessian. (b) Trajectories of the QRNPO algorithm (Talebi and Mesbahi, 2022) using Riemannian Hessian in blue, incorporating the curvature, versus the Euclidean Hessian in orange, where the former takes more efficient trajectories towards the global minimum (denoted by the red star).

This result enables us to obtain explicit formulae for the Riemannian gradient and Hessian of any smooth costs on \mathcal{S} when restricted to $\tilde{\mathcal{S}} = \mathcal{S} \cap \mathcal{K}$. In fact, this is proved for any embedded submanifold of an abstract Riemannian manifold. As expected, these geometric derivatives will be affected by the curvature of $(\mathcal{S}, \langle \cdot, \cdot \rangle^L)$ which is accurately captured by the second term of the Weingarten mapping. In explicit form, these can be computed using the Christoffel symbols associated with induced Levi-Civita connection ∇ ; see (Talebi and Mesbahi, 2023, Prop. 3.4) for the general proof and explicit formulae of these quantities.

By direct application of these results to the constraint LQR cost $\tilde{J}_{\text{LQR}} := J_{\text{LQR}}|_{\tilde{\mathcal{S}}}$, we can give explicit formulae for Riemannian gradient and Hessian:

$$\begin{aligned} \text{grad } \tilde{J}_{\text{LQR}}(K) &= \pi^\top (RK + B^\top P_K A_{\text{cl}}) \\ \bar{\nabla} \tilde{J}_{\text{LQR}}(K) &= \text{Proj}_K((RK + B^\top P_K A_{\text{cl}})Y_K), \end{aligned}$$

where Proj_K is the ordinary Euclidean projection operator from $T_K \mathcal{S}$ onto $T_K \tilde{\mathcal{S}}$. Similarly, the Riemannian, Euclidean, and Pseudo-Euclidean Hessians for $\tilde{J}_{\text{LQR}}(\cdot)$ can be obtained.

In Figure 6, we provide a numerical illustration of how this Riemannian metric is useful, and how the curvature information enables more efficient algorithms.⁶

4.4. Linear Quadratic Gaussian (LQG) Control

In this subsection, we move to discuss the geometry in policy optimization for LQG control (16). As we will see below, while sharing certain similarities, the non-convex LQG landscape is richer and more complicated than the LQR case.

⁶The figure pertains to the example as in Figure 2, where the feedback gain is constrained to be diagonal.

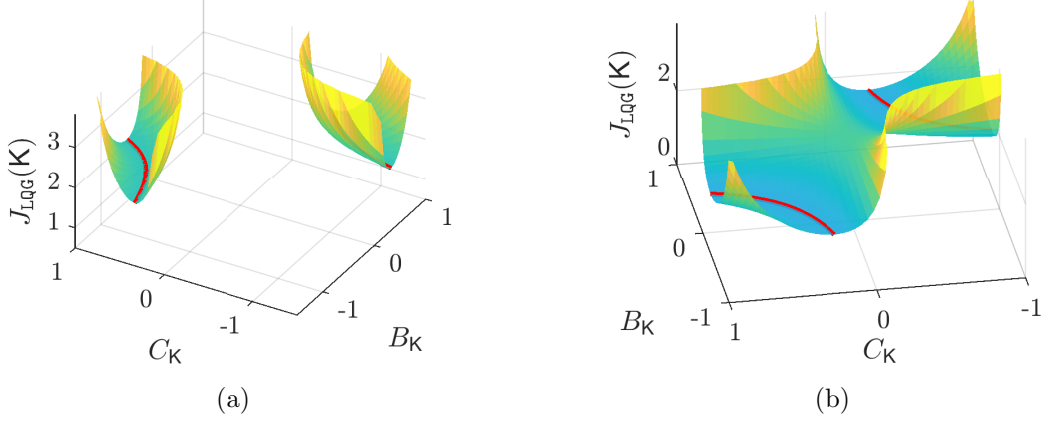


Figure 7: Non-isolated and disconnected optimal LQG policies (highlighted by the red curves). In both cases, we set $Q = 1, R = 1, V = 1, W = 1$. (a) LQG cost for the open-loop unstable system with $A = 1.1, B = C = 1$, where we fixed $A_K = -0.3069$; (b) another LQG cost for the open-loop stable system with $A = 0.9, B = C = 1$, where we fixed $A_K = -0.1753$. In (b), the origin $B_K = 0, C_K = 0$ with $A_K = -0.1753$ is a saddle point.

Recall that the set of stabilizing policies \mathcal{C}_n has at most two path-connected components that are diffeomorphic to each other under a particular similarity transformation (Fact 3.4). As similarity transformations do not change the input/output behavior of dynamic policies, it makes no difference to search over any path-connected component even if \mathcal{C}_n is not path-connected. This feature brings positive news for local policy search algorithms over dynamic stabilizing policies \mathcal{C}_n .

4.4.1. Spurious Stationary Points and Global Optimality

Similar to the LQR case, for any stabilizing policy $\mathbf{K} \in \mathcal{C}_n$, the LQG cost function $J_{\text{LQG}}(\mathbf{K})$ in (16) has the following expressions:

$$J_{\text{LQG}}(\mathbf{K}) = \text{tr} \left(\begin{bmatrix} Q & 0 \\ 0 & C_K^T R C_K \end{bmatrix} X_K \right) = \text{tr} \left(\begin{bmatrix} W & 0 \\ 0 & B_K V B_K^T \end{bmatrix} Y_K \right), \quad (33)$$

where X_K and Y_K are the unique positive semidefinite solutions to the Lyapunov equations below

$$X_K = \begin{bmatrix} A & B C_K \\ B_K C & A_K \end{bmatrix} X_K \begin{bmatrix} A & B C_K \\ B_K C & A_K \end{bmatrix}^T + \begin{bmatrix} W & 0 \\ 0 & B_K V B_K^T \end{bmatrix}, \quad (34a)$$

$$Y_K = \begin{bmatrix} A & B C_K \\ B_K C & A_K \end{bmatrix}^T Y_K \begin{bmatrix} A & B C_K \\ B_K C & A_K \end{bmatrix} + \begin{bmatrix} Q & 0 \\ 0 & C_K^T R C_K \end{bmatrix}. \quad (34b)$$

Note that X_K and Y_K are closely related to the controllable and observable Gramians of the closed-loop system (14).

From (33), it is not difficult to see that $J_{\text{LQG}}(\mathbf{K})$ is a rational function in terms of the policy parameter \mathbf{K} , and it is thus a real analytic on \mathcal{C}_n . We summarize this as a fact below.

Fact 4.1. The LQG cost $J_{\text{LQG}}(\mathbf{K})$ in (16) is real analytic on \mathcal{C}_n , and in particular smooth.

It is also easy to identify examples to confirm the non-convexity of LQG policy optimization (16) (note that the domain \mathcal{C}_n is already non-convex; see Figure 3). Unlike the LQR, it is known that the problem of LQG problem (16) has non-unique and non-isolated globally optimal policies

in the state-space form \mathcal{C}_n . This is not difficult to see since any similarity transformation on one optimal LQG policy \mathbf{K}^* leads to another optimal solution that achieves the same cost, i.e.,

$$J_{\text{LQG}}(\mathbf{K}^*) = J_{\text{LQG}}(\mathcal{T}_T(\mathbf{K}^*)), \quad \forall T \in \text{GL}_n. \quad (35)$$

Figure 7 illustrates the non-convex LQG landscape and the non-isolated/disconnected optimal LQG policies. It is also known that the LQG cost J_{LQG} is not coercive: there might exist sequences of stabilizing policies $\mathbf{K}_j \in \mathcal{C}_n$ where $\lim_{j \rightarrow \infty} \mathbf{K}_j \in \partial \mathcal{C}_n$ such that $\lim_{j \rightarrow \infty} J_{\text{LQG}}(\mathbf{K}_j) < \infty$, and sequences of stabilizing policies $\mathbf{K}_j \in \mathcal{C}_n$ where $\lim_{j \rightarrow \infty} \|\mathbf{K}_j\|_F = \infty$ such that $\lim_{j \rightarrow \infty} J_{\text{LQG}}(\mathbf{K}_j) < \infty$. The latter fact is easy to see from the effect of similarity transformation (35) since $J_{\text{LQG}}(\mathbf{K})$ is constant for policies that are connected by any $T \in \text{GL}_n$; also see (Zheng et al., 2023, Example 4.1) for the former fact. A closed-form expression for the gradient of the LQG cost function $\bar{\nabla} J_{\text{LQG}}$ can also be obtained; see Zheng et al. (2023) for details.

As shown in Figure 7, the set of stationary points $\{\mathbf{K} \in \mathcal{C}_n \mid \bar{\nabla} J_{\text{LQG}}(\mathbf{K}) = 0\}$ is not isolated and can be disconnected. Furthermore, there may exist strictly suboptimal spurious stationary points for the LQG control (16). This fact can be seen from Figure 7(b), in which the policy $\mathbf{K} \in \mathcal{C}_1$ with values $A_{\mathbf{K}} = -0.1753$, $B_{\mathbf{K}} = 0$, and $C_{\mathbf{K}} = 0$ corresponds to a saddle point. Indeed, the following result explicitly characterizes a class of saddle points in LQG control (16) when the plant dynamics are open-loop stable. These stationary points are spurious and suboptimal whenever the globally optimal LQG policy corresponds to a nonzero transfer function.

Fact 4.2 (Saddle points in LQG). Suppose (11) is open-loop stable. Let $A_{\mathbf{K}} = \Lambda \in \mathbb{R}^{n \times n}$ be any stable matrix. Then the zero policy $\mathbf{K} \in \mathcal{C}_n$ with parameters $A_{\mathbf{K}} = \Lambda, B_{\mathbf{K}} = \mathbf{0}, C_{\mathbf{K}} = \mathbf{0}$ is a stationary point of $J_{\text{LQG}}(\mathbf{K})$ over \mathcal{C}_n , and the corresponding Hessian is either indefinite or zero.

Due to the existence of spurious saddle points, LQG policy optimization (16) cannot enjoy the gradient dominance property as the LQR case. The gradient dominance property will also fail for the LQG control even when an observer-based policy parameterization is used (Mohammadi et al., 2021b). Note that the policy \mathbf{K} in Fact 4.2 corresponds to a zero transfer function, and the policy just produces a zero input. It has been shown that *all spurious stationary points \mathbf{K} are non-minimal dynamic policies*, i.e., either $(A_{\mathbf{K}}, B_{\mathbf{K}})$ is not controllable, or $(C_{\mathbf{K}}, A_{\mathbf{K}})$ is not observable or both. Therefore, we have the following result about globally optimal LQG policies.

Fact 4.3 (Global optimality in LQG). All stationary points that correspond to controllable and observable policies are globally optimal in the LQG problem (16). These globally optimal policies are related to each other by a similarity transformation.

The proof is based on closed-form gradient expressions for controllable and observable stationary points $\mathbf{K} \in \mathcal{C}_n$ (by letting the gradients equal to zero), which are shown to be the same as the optimal solution from Riccati equations. This proof strategy was first used in (Hyland and Bernstein, 1984) to derive first-order necessary conditions for optimal reduced-order controllers. It strongly depends on the assumption of minimality, which fails to deal with non-minimal globally optimal policies for LQG control. Beyond minimal policies, a recent extension of global optimality characterization in LQG control is (Zheng et al., 2023, Theorem 4.2), which is based on a notion of *non-degenerate* stabilizing policies. This characterization relies on a more general strategy of extended convex lifting that captures a suitable convex re-parameterization of LQG control (16).

4.4.2. Invariances of LQG: a Quotient Geometry

This subsection is a sequel to the quotient manifold setup introduced in §3.3. Recall the LQG cost J_{LQG} solely depends on the input-output properties of the closed loop system. If our

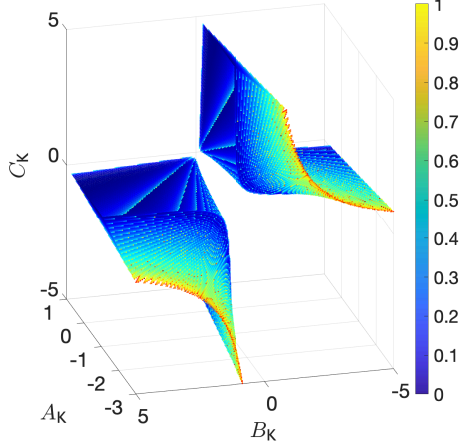


Figure 8: A colored plot of the LQG cost $J_{\text{LQG}}(\cdot)$ over \mathcal{C}_n with $A = 1.1, B = C = 1$. Color is determined via an affine transformation of $\log(J_{\text{LQG}}(\mathbf{K}))$ so that the minimum LQG cost is mapped to 0 and the maximum LQG cost is mapped to 1, over the given plot bounds on A_K, B_K, C_K .

parameterization of choice is the state-space form in (15), then the control design objective will be invariant under similarity transformation: $J_{\text{LQG}}(\mathbf{K}_1) = J_{\text{LQG}}(\mathbf{K}_2)$, for any $\mathbf{K}_1, \mathbf{K}_2 \in \mathcal{C}_n$ lying in the same orbit $[\mathbf{K}_1] = [\mathbf{K}_2]$. Figure 8 shows an example of such LQG cost on \mathcal{C}_1 ; also compare with the orbits plotted in Figure 4.

The similarity-invariance of LQG causes many hindrances for policy optimization. First, each stationary point lies within an orbit of stationary points, and this orbit will have dimension n^2 . Therefore, the Hessian of any stationary point will be singular: its nullspace dimension will be at least n^2 . This may muddle the policy optimization algorithms. Also, local convergence guarantees will be more difficult to obtain since the Hessian at the global minimum cannot be positive-definite.

Second, since the group product is not coordinate-invariant, we lose the useful invariance property:

$$\bar{\nabla} J_{\text{LQG}}(\mathcal{T}_T(\mathbf{K})) \neq \mathcal{T}_T(\bar{\nabla} J_{\text{LQG}}(\mathbf{K})).$$

This has impacts on the initialization: if we choose a particularly bad initialization $\|K_0\|_F \gg 0$, then we will always have $\|\bar{\nabla} J_{\text{LQG}}(\mathbf{K})\|_F \gg 0$. This also implies that gradient descent fails to satisfy the following property known as similarity-equivariance:

$$\mathcal{T}_T(\mathbf{K} - \alpha \bar{\nabla} J_{\text{LQG}}(\mathbf{K})) \neq \mathcal{T}_T(\mathbf{K}) - \alpha \bar{\nabla} J_{\text{LQG}}(\mathcal{T}_T(\mathbf{K})). \quad (36)$$

As we will see, we can resolve these issues by introducing a similarity-invariant Riemannian metric and devising a Riemannian gradient descent procedure.

Since $J_{\text{LQG}}(\cdot)$ is similarity-invariant, we can induce a unique cost onto the smooth quotient space $\mathcal{C}_n/\text{GL}_n$ as follows:

$$\tilde{J}_{\text{LQG}}([\mathbf{K}]) := J_{\text{LQG}}(\mathbf{K}')$$

where \mathbf{K}' is any controller $\mathbf{K}' \in [\mathbf{K}]$. Now let us equip \mathcal{C}_n^{\min} with the KM metric (22) and $\mathcal{C}_n^{\min}/\text{GL}_n$ with the induced quotient metric. Then the Riemannian gradient is similarity-equivariant:

$$\text{grad } J_{\text{LQG}}(\mathcal{T}_T(\mathbf{K})) = \mathcal{T}_T(\text{grad } J_{\text{LQG}}(\mathbf{K}))$$

Using the Euclidean retraction, which is similarity-equivariant, we therefore have the fact that a single step of Riemannian gradient descent is similarity equivariant; that is,

$$\mathcal{T}_T(\mathbf{K} - \alpha \text{grad } J_{\text{LQG}}(\mathbf{K})) = \mathcal{T}_T(\mathbf{K}) - \alpha \text{grad } J_{\text{LQG}}(\mathcal{T}_T(\mathbf{K})).$$

This is a remarkable property. If we perform a similarity transformation on the initial controller \mathbf{K}_0 , then the resulting sequence of iterates will also be transformed by that same similarity transformation.

This also implies the following. Let $\mathbf{K} \in \mathcal{C}_n^{\min}$ and consider $\mathbf{K}^+ := \mathbf{K} - \alpha \text{grad } J_{\text{LQG}}(\mathbf{K})$. Let $x := [\mathbf{K}] \in \mathcal{C}_n^{\min}/\text{GL}_n$ and define $x^+ := \mathcal{R}_x(-\alpha \text{grad } \tilde{J}_{\text{LQG}}(x))$. Then $x^+ = [\mathbf{K}^+]$. In other words, Riemannian gradient descent over the Riemannian quotient manifold coincides with Riemannian gradient descent over the total manifold. We emphasize that these properties hold only when the Riemannian metric is similarity-invariant (20), such as the KM metric, and the retraction is similarity-*equivariant*, such as the Euclidean retraction.

We will end this section with a lemma that shows how this setup reduces the nullspace dimension of Riemannian Hessian at stationary points. The following result quantifies the number of eigenvalues of the Riemannian Hessian with positive, zero, and negative signs—referred to as its “signature.”

Fact 4.4. Let \mathcal{M} be a manifold under group action G equipped with a G -invariant Riemannian metric. Suppose \mathcal{M}/G is a smooth quotient manifold and consider any G -invariant smooth function $J : \mathcal{M} \rightarrow \mathbb{R}$. If (n_-, n_0, n_+) is the signature of $\text{Hess } J(x^*)$ at any stationary point $x^* \in \mathcal{M}$ of J , then the signature of $\text{Hess } \tilde{J}([x^*])$ is $(n_-, n_0 - \dim(G), n_+)$, where $\tilde{J}([x]) := J(x)$.

To illustrate a consequence of this lemma, suppose \mathbf{K}^* is a global minimum of J_{LQG} . This implies $\bar{\nabla}^2 J_{\text{LQG}}(\mathbf{K}^*)$ has at least q^2 zero eigenvalues. Then, due to the lack of positive-definiteness of the Hessian, iterative updates may not be guaranteed with a linear rate of convergence. But, by this shows that $\text{Hess } \tilde{J}_{\text{LQG}}([\mathbf{K}^*])$ has q^2 less zeros. So, if $\dim \ker \bar{\nabla}^2 J_{\text{LQG}}(\mathbf{K}^*) = q^2$ then $\text{Hess } \tilde{J}_{\text{LQG}}([\mathbf{K}^*]) > 0$ which is the property that enables a local linear rate of convergence guaranteed in (Kraisler and Mesbahi, 2024, Thm. 5.2) for the continuous system dynamics.

4.5. \mathcal{H}_∞ -norm: Systems with Adversarial Noise

In this section, we return to the state-feedback \mathcal{H}_∞ optimal control problem introduced in §2.2.3. Setting the initial state $x_0 = 0$ and considering a stabilizing policy $K \in \mathcal{S}$, the \mathcal{H}_∞ performance $J_\infty(\cdot)$ coincides with the square of the \mathcal{H}_∞ norm of the closed-loop transfer function from w_t to a performance measure $z_t := [(Q^{1/2}x_t)^\top \quad (R^{1/2}u_t)^\top]^\top$. Explicitly,

$$\begin{aligned} J_\infty(K) &= \sup_{\|w\|_{l_2} \neq 0} \frac{\|z\|_{l_2}^2}{\|w\|_{l_2}^2} = \left\| \begin{bmatrix} Q^{1/2} \\ R^{1/2}K \end{bmatrix} (zI - A - BK)^{-1} \right\|_\infty^2 \\ &= \sup_{\omega \in [0, 2\pi]} \lambda_{\max} \left((e^{-j\omega} - A - BK)^{-\top} (Q + K^\top R K) (e^{j\omega} - A - BK)^{-1} \right), \end{aligned} \quad (37)$$

where $\lambda_{\max}(\cdot)$ denotes the maximal eigenvalue of an Hermitian matrix.

Unlike the case of LQR or LQG, we usually do not have a closed-form expression to evaluate the \mathcal{H}_∞ norm (37). One can also use the celebrated KYP lemma to evaluate it using a linear matrix inequality (LMI), but the solution can take more computational efforts than its counterparts in LQR (29) or LQG (33) that only involve solving (linear) Lyapunov equations. Classical control techniques typically re-parameterize the non-convex \mathcal{H}_∞ control (17) into a convex LMI

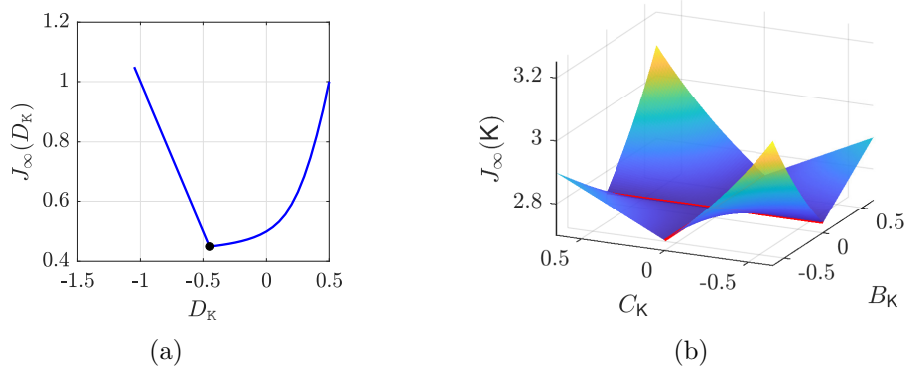


Figure 9: Non-convexity and non-smoothness of the \mathcal{H}_∞ cost function. (a) illustrates a static output feedback \mathcal{H}_∞ control instance with $u_t = D_K y_t$ which shows one non-smooth point (highlighted by the black point); (b) corresponds to a dynamic \mathcal{H}_∞ control instance which exhibits a set of nonsmooth points (highlighted by the red lines); see (Zheng et al., 2023, Example 5.1) for further details.

via a change of variables (Boyd et al., 1994), or directly characterize a suboptimal solution via solving a single (quadratic) Riccati equation (Zhou and Khargonekar, 1988). Here, we discuss some geometric aspects of the \mathcal{H}_∞ policy optimization (17).

Compared with the LQR and LQG, one major difference in \mathcal{H}_∞ control is that the function $J_\infty(K)$ in (37) is non-smooth, i.e., the cost function $J_\infty(K)$ may not be differentiable at some feasible points $K \in \mathcal{S}$ (see Figure 9 for an illustration). This fact is actually not difficult to see due to two possible sources of non-smoothness in (37): One from taking the largest eigenvalue of complex matrices, and the other from maximization over $\omega \in [0, 2\pi]$. Indeed, robust control problems were one of the early motivations and applications for non-smooth optimization (Lewis, 2007). Despite the non-smoothness, the \mathcal{H}_∞ cost function is *locally Lipschitz* and thus differentiable almost everywhere (Figure 9 also illustrates this). Thus, we can define the Clarke directional derivative and Clarke subdifferential of $J_\infty(K)$ at each feasible policy $K \in \mathcal{S}$.

Furthermore, the \mathcal{H}_∞ cost function $J_\infty(K)$ is known to be “subdifferentially regular” in the sense of Clarke (Clarke, 1990) (i.e., the ordinary directional derivative exists and coincides with the Clarke directional derivative for all directions). Also, it is known that the discrete-time state-feedback \mathcal{H}_∞ cost function (37) is coercive. We summarize these properties property below, which to some extent are analogous to those of LQR cost in Lemma 4.3.

Lemma 4.5. *Suppose $Q \succ 0, R \succ 0$ and (A, B) is stabilizable. Then, the \mathcal{H}_∞ cost function $J_\infty: \mathcal{S} \mapsto \mathbb{R}$, defined in (37),*

- (a) *is locally Lipschitz, and thus almost everywhere differentiable;*
- (b) *is subdifferentially regular over the set of stabilizing policies \mathcal{S} ;*
- (c) *is coercive⁷: $K \rightarrow \partial\mathcal{S}$ or $\|K\| \rightarrow \infty$ each implies $J_\infty(K) \rightarrow \infty$;*
- (d) *has compact, path-connected sublevel sets $\mathcal{S}_\gamma = \{K \in \mathcal{S} \mid J_\infty(K) \leq \gamma\}$ for any $\gamma \geq \gamma^* := \min_K J_\infty(K)$.*

⁷We remark that this coerciveness property fails to hold in the continuous-time state-feedback \mathcal{H}_∞ control, even when $Q \succ 0, R \succ 0$; see (Zheng et al., 2024, Fact 4.1)

The proof idea for the first two properties is to view $J_\infty(K)$ as a composition of a convex mapping $\|\cdot\|_\infty$ and the mapping from K to a stable closed-loop transfer function that is continuously differentiable over \mathcal{S} . In the discrete time, the coerciveness of J_∞ can be proved using the positive definiteness of Q and R . The compactness of sublevel sets follows directly by coercivity. The sublevel set \mathcal{S}_γ is in general non-convex but always path-connected. One can also compute the set of subdifferential $\partial J_\infty(K)$ at each feasible policy $K \in \mathcal{S}$; however, the computation is much more complicated than the smooth LQR or LQG case. We refer the interested reader to (Zheng et al., 2023, Lemma 5.2) and Apkarian and Noll (2006a) for more details. Despite the non-convex and non-smoothness, we have a global optimality characterization for (17).

Fact 4.5 (Global optimality in \mathcal{H}_∞ control). Consider the state-feedback \mathcal{H}_∞ control (17) with $Q \succ 0, R \succ 0$. Any Clarke stationary point is globally optimal.

The high-level proof of the above results proceed as follows: it is known that (17) admits an equivalent convex reformulation by a change of variables, and this change of variables can be designed as a diffeomorphism between non-convex policy optimization and its convex reformulation; this diffeomorphism then allows us to certify global optimality in original non-smooth and non-convex \mathcal{H}_∞ control; see (Guo and Hu, 2022, Theorem 1) and (Zheng et al., 2024, Corollary 4.1) for details. This idea has further been characterized into a framework of extended convex lifting (ECL) in (Zheng et al., 2023, 2024), which bridges the gap between non-convex policy optimization and convex reformulations in a range of control problems.

5. Algorithmic Implications

In the context of reinforcement learning and control, geometric perspectives on policy optimization facilitate the development of data-driven algorithms that can emulate various first- and second-order policy iteration schemes. These approaches typically involve synthesizing a first- or second-order oracle using available performance measure information. This framework provides a basis for comparing the data efficiency of different techniques in terms of sample complexity. Specifically, it addresses how many function calls to the oracle are necessary to achieve the desired level of optimality when the algorithm has access only to the oracle rather than the explicit problem parameters.

5.1. Convergence of Policy Optimization Algorithms

Despite the non-convexity of the LQR problem in the policy parameters K , the analysis of the domain manifold and the properties of LQR cost in §4.3.1, in particular the gradient dominance property has enabled establishing the following global linear convergence guarantees of gradient descent algorithms (Fazel et al., 2018a; Bu et al., 2019). This linear convergence result is mainly due to the *coerciveness*, *smoothness* over any sublevel set, and *gradient dominance* of the LQR cost function $J_{\text{LQR}}(K)$ (see Lemma 4.3).

Fact 5.1. Starting from any feasible $K_0 \in \mathcal{S}$, a small enough (but constant) step-size η remains stabilizing for the gradient descent updates $K^+ = K - \eta \bar{\nabla} J_{\text{LQR}}(K)$ which converges to the optimal LQR policy K^* at a linear rate.

As discussed in Remark 1, the algebraic update of Hoyer’s algorithm can be described as a “Riemannian quasi-Newton” update and we can provide an alternative proof for its global convergence Talebi and Mesbahi (2023).

Fact 5.2. Starting from any feasible $K_0 \in \mathcal{S}$, the unit step size remains stabilizing for the Hewer’s update $K^+ = K + \hat{V}$ with \hat{V} solving $\hat{H}_K \hat{V} = -\text{grad } J_{\text{LQR}}(K)$ which converges to the optimal LQR policy K^* at a quadratic rate.

In the specific context of Hewer’s update, the input-output system trajectory can be directly utilized to obtain a positive definite approximation of the Riemannian Hessian \hat{H}_K and the Riemannian gradient $\text{grad } J_{\text{LQR}}(K)$ through a recursive least squares scheme [Bradtke et al. \(1994\)](#). This approach can be extended to solve constrained LQR problems, as demonstrated in [Alemzadeh et al. \(2024\)](#), which focuses on learning policies that adhere to a communication/information graph in a large network of homogeneous systems. Extensions to any linearly constrained policies, including static output feedback and structured LQR problems, utilizing the stability certificate idea in [Lemma 4.1](#) are explored in [Talebi and Mesbahi \(2023\)](#) and summarized below:

Fact 5.3. Starting from any feasible $K_0 \in \tilde{\mathcal{S}} = \mathcal{S} \cap \mathcal{K}$, the stepsize $\eta_K = \min(1, s_K)$ remains stabilizing for the Riemannian Newton update $K^+ = K + \eta_K V_K$ with V_K solving $\text{Hess } J_{\text{LQR}}|_K(V_K) = -\text{grad } J_{\text{LQR}}(K)$ and its variants (by replacing Hess with $\overline{\text{Hess}}$). Furthermore, any non-degenerate local minimum is contained in a neighborhood on which the generated sequence of policies remains therein and converges to the local minimum fast—at a linear rate that eventually becomes quadratic.

Inspired by this result, recently an online optimistic version of these updates are studied in [Chang and Shahrampour \(2024\)](#) with regret bound guarantees.

Let us move to the policy optimization for LQG control [\(16\)](#) over the dynamic output-feedback policies \mathcal{C}_n . Despite being non-convex, the geometrical properties of \mathcal{C}_n and the LQG cost function $J_{\text{LQG}}(\cdot)$ (in [§4.4](#)) can ensure some favorable properties of policy gradient algorithms. While the feasible region \mathcal{C}_n can be path-connected, [Fact 3.4](#) ensures that the two path-connected components are identical from an input-output perspective. Thus, when applying policy search algorithms to solve LQG problem [\(16\)](#), it makes no difference to search over either path-connected component. In addition, if a sequence of gradient iterates converges to a point, [Fact 4.3](#) further allows us to verify whether the limit point is a globally optimal solution to the LQG control [\(16\)](#). The following is an immediate corollary of this fact.

Fact 5.4. Consider a gradient descent algorithm $K_{t+1} = K_t - \alpha_t \overline{\nabla} J_{\text{LQG}}(K_t)$ for the LQG problem [\(16\)](#), where α_t is a step size. Suppose $\inf_t \alpha_t > 0$ and the iterates K_t converge to a point K^* . Then K^* is globally optimal if it is a minimal controller.

We emphasize that there are two major limitations in [Fact 5.4](#): 1) it does not address the case when the limit point has a vanishing gradient ($\overline{\nabla} J_{\text{LQG}}(K^*) = 0$) but is non-minimal; 2) it does not offer conditions to ensure convergence of the gradient descent iterates. Indeed, [Fact 4.2](#) has revealed that there may exist strictly suboptimal saddle points for non-minimal LQG policies in [\(16\)](#). If a stationary point does not correspond to a minimal (aka, controllable and observable) policy, we cannot confirm optimality. Furthermore, some saddle points are *high-order* in the sense that they have degenerate Hessian (e.g., the corresponding Hessian is zero), and thus there is no escaping direction that is a key element in the developments on perturbed gradient methods to avoid saddles ([Jin et al., 2017](#)). Recently, [Zheng et al. \(2022\)](#) introduced a new perturbed policy gradient (PGD) algorithm to escape a class of spurious stationary points (including high-order saddles). One key idea is to use a novel reparameterization procedure that converts the iterate from a high-order saddle to a strict saddle, from which standard random perturbations in gradient descent can escape efficiently.

The inherent symmetry induced by similarity transformation still makes the convergence conditions of ordinary gradient descent methods hard to derive. With the Riemannian quotient manifold setup $\mathcal{C}_n^{\min}/\text{GL}_n$ in §4.4.2, a local linear convergence rate for Riemannian gradient methods is derived in [Kraisler and Mesbahi \(2024\)](#)—whenever the iterates are close to a globally optimal policy. We summarize this result as follows.

Fact 5.5. Let $\mathcal{C}_n^{\min}/\text{GL}_n$ be the orbit space of full-order minimal dynamic feedback controllers (for the continuous LTI dynamics) modulo similarity transformation. Under certain regularity conditions on J_{LQG} ([Kraisler and Mesbahi, 2024](#), Assumption 5.1), let \mathbf{K}^* be an optimal LQG controller. Consider the Riemannian gradient descent updates under the KM metric $\langle \cdot, \cdot \rangle^{\text{KM}}$ and the Euclidean retraction, written as $\mathbf{K}_{t+1} = \mathbf{K}_t - \alpha \text{grad } J_{\text{LQG}}(\mathbf{K}_t)$ with a sufficiently small step size $\alpha > 0$. Then, there exists a neighborhood of $[\mathbf{K}^*]$ in which if we initialize $\mathbf{K}_0 \in [\mathbf{K}^*]$, then $\lim_{t \rightarrow \infty} [\mathbf{K}_t] = [\mathbf{K}^*]$. That is, the orbit of $[\mathbf{K}]$ converges to the orbit of $[\mathbf{K}^*]$. Furthermore, the rate of convergence is linear.

5.2. Oracle-based Data-driven Algorithms

The discussions in §5.1 require exact (Riemannian) gradient information. In model-free scenarios, it is possible to evaluate the performance measure $J(\theta)$ for a given set of policy parameters θ that determines an input $\mathbf{u} = \pi_\theta(\mathbf{x})$. As will become clear in the following discussion, it is reasonable to construct oracles based on these function evaluations, which may differ depending on the specific method used for gradient estimation. This approximate evaluation of $J(\theta)$ is feasible whenever its explicit form is known and the system’s input-output trajectory (\mathbf{u}, \mathbf{y}) can be obtained through independent experiments. Like other sample-based techniques, the performance of each approximation can be quantified by evaluating the bias-variance trade-off, which directly impacts the probabilistic convergence guarantees of these methods.

Probably the most natural of these approaches is the Finite Difference Method, where the gradient is estimated by relating it back to the performance difference of randomly selected perturbations in the d -dimensional policy parameters $\theta \in \Theta$ through smoothing techniques. In particular, one may approximate $J(\theta)$ by the following averaging/smoothing:

$$J(\theta) \approx \hat{J}(\theta) := \mathbb{E}_{\nu \sim \text{Uni}\{\mathbb{B}^d\}} J(\theta + \varepsilon\nu),$$

where \mathbb{B}^d denotes the unit d -dimensional ball and ε is a small radius. Then, the gradient can be approximated by ([Flaxman et al., 2004](#), Lemma 1):

$$\bar{\nabla} \hat{J}(\theta) = \mathbb{E}_{U \sim \text{Uni}\{\mathbb{S}^d\}} \left[\frac{J(\theta + \varepsilon U) - J(\theta - \varepsilon U)}{2\varepsilon/d} U \right],$$

where \mathbb{S}^d denotes the unit d -dimensional sphere. In line with this, the so-called two-point approximation from finite samples can be expressed as [Spall \(1998\)](#):

$$\bar{\nabla} \hat{J}(\theta) = \frac{1}{N} \sum_{i=1}^N \frac{J(\theta + \varepsilon U_i) - J(\theta - \varepsilon U_i)}{2\varepsilon/d} U_i,$$

where U_i is a (feasible) randomly selected unit vector, ε is a small enough perturbation parameter, and N is the number of samples. Note that if the perturbation size is particularly small, we can ensure the feasibility of the perturbed policy $\theta + \varepsilon U$, especially when Θ has a relatively open structure, as in the case of the set of static/constrained/dynamic stabilizing policies \mathcal{S} , $\tilde{\mathcal{S}}$, or \mathcal{C}_q .

For data efficiency, the two-point approximation can be further reduced to the so-called one-point approximation as follows [Flaxman et al. \(2004\)](#):

$$\bar{\nabla}_\theta \hat{J}(\theta) \approx \frac{1}{N} \sum_{i=1}^N \frac{J(\theta + \varepsilon U_i)}{\varepsilon/d} U_i.$$

These estimations, for example, enables learning optimal LQR policy from input output trajectories with (probabilistic) global convergence guarantees [Fazel et al. \(2018a\)](#).

Similarly, analogous arguments can be followed to estimate the Hessian of the cost from additional independent samples ?. However, these techniques often lead to high variance issues, which can be mitigated by introducing an initial state-dependent “baseline” $J(\theta; x_0)$ for approximating these variations [Grondman et al.; Kakade \(2001\)](#):

$$\bar{\nabla}_\theta \hat{J}(\theta) \approx \frac{1}{N} \sum_{i=1}^N \frac{J(\theta + \varepsilon U_i; x_0^i) - J(\theta; x_0^i)}{\varepsilon/d} U_i,$$

where the baseline is independently approximated by $J(\theta; x_0^i) = \mathbb{E}_{U \sim \text{Uni}\{\mathbb{S}^d\}} \left[\frac{J(\theta + \varepsilon U)}{\varepsilon/d} U \right]$ for each initial state x_0^i . This technique is adopted, for example, in [Takakura and Sato \(2024\)](#) to reducing variance of learning output feedback LQR policy. A similar approach can be applied for Hessian approximation.

It is also worth noting that these data generation procedures for model-free function evaluation, often require *a priori* access to a stabilizing policy for the underlying system dynamics. This relates to online stabilization problems and its intricate geometry from its fundamental limitations [Talebi et al. \(2022\)](#) to algorithm design; see for example [Yu et al. \(2023\)](#).

5.3. Optimal Estimation Problems

Another recent development has seen the translation of policy optimization techniques, originally developed for optimal control, to optimal estimation problems through the profound “duality relation” between these two setups [Talebi et al. \(2023\)](#). In the optimal estimation context, the mean-squared estimation (MSE) error can be naturally expressed as an average

$$J_{\text{MSE}}(\theta) = \mathbb{E}_{\mathbf{y}} \text{SE}(\theta, \mathbf{y}),$$

where $\text{SE}(\theta, \mathbf{y})$ denotes the squared estimation error. The gradient of this error can be computed for any observed trajectory \mathbf{y} and given (now called) estimation policy θ . This gradient, $\bar{\nabla}_\theta \text{SE}(\theta, \mathbf{y})$, can be approximated using finite-length output trajectories \mathbf{y}_T . This results in a natural gradient approximation scheme based on N finite-length output trajectories as follows:

$$\bar{\nabla} J_{\text{MSE}}(\theta) \approx \bar{\nabla} \hat{J}_T(\theta) = \frac{1}{N} \sum_{i=1}^N \bar{\nabla}_\theta \text{SE}(\theta, \mathbf{y}_T^i).$$

Finally, an analysis of the bias-variance trade-off enables the establishment of probabilistic guarantees for the convergence of Stochastic Gradient Descent (SGD) for θ to the optimal Kalman estimation policy [Talebi et al. \(2023\)](#):

Fact 5.6. Suppose the system is observable and both dynamic and measurement noise are bounded. Consider the stochastic gradient descent on the estimation policy $\theta^+ = \theta - \eta \bar{\nabla} \hat{J}_T(\theta)$ with small enough stepsize η . Then, with high probability, it converges linearly and globally (from any initial stabilizing policy) to the optimal Kalman estimation policy.

5.4. Broader Implications: Iterative Learning Procedures

Other policy parameterization techniques have seen significant success over the last couple of decades, particularly through Linear Matrix Inequality (LMI) techniques, which enable the formulation of stability, robustness, and other performance considerations. These approaches often rely on parameterizing policies in specific ways, such as Youla parameterization, which can be heavily dependent on the underlying system model.

However, these “model-dependent formulations”, such as those involving Riccati equations and LMI techniques, have limitations when it comes to generalizing across nonlinear dynamics and complex policy parameterizations. In contrast, the complete policy optimization approach offers greater generalization power, particularly for nonlinear dynamics and policies, such as those using neural networks. Additionally, it simplifies the imposition of direct constraints on the synthesized input signal. Incorporating such constraints within those model-dependent frameworks is not straightforward, making the complete policy optimization approach more versatile and robust for a broader range of applications.

6. Summary and Outlook

In this survey, we have provided an overview of recent progress on understanding geometry of policy optimization and its algorithmic implications. This has been pursued both in terms of the static and dynamic stabilization problems, as well as the how control performance objectives interact with this set. The implications of such geometric perspective on policy optimization for developing first order methods for control design, as well as their model-free data driven realizations are also discussed.

Some of key ideas that underlie our presentation include developing a geometric machinery to reason about fundamental (complexity) bounds for feedback design, both in terms of model parameters as well as available data. For example, we advocate that understanding the geometry of the cost, when constrained to submanifolds of stabilizing feedback gains, is crucial for devising efficient model-based and model-free algorithms for robust and optimal designs, be it in terms of homotopies, escaping saddle points, conditioning, or effective use of symmetries.

7. Notes and Commentary

Throughout this manuscript, we reference (Lee, 2018) for standard geometric notions such as Riemannian metric, connection, vector field, gradient, Hessian, and Weingarten mapping. In §3, the topological properties of static stabilizing policies are from (Bu et al., 2021), with earlier results in (Ohara and Amari, 1992a; Fam and Meditch, 1978; Ober, 1987). For static state-feedback Hurwitz stabilizing policies in continuous-time LTI systems, see (Ohara and Amari, 1992b). The geometric PO ideas on SLQR and Output-feedback Linear Quadratic Regulators (OLQR) are reviewed from (Talebi and Mesbahi, 2022), and further details on the gradient, Hessian, and Christoffel symbols are in (Talebi and Mesbahi, 2023).

The results in on dynamic feedback synthesis for LQG in Section 4.4 are based on (Tang et al., 2023; Kraiser and Mesbahi, 2024), and other related results can be found in (Duan et al., 2024; Hu and Zheng, 2022). The topological properties of stabilizing dynamic feedback policies are discussed in (Tang et al., 2023), with Fact 3.4 adapted from (Tang et al., 2023, Theorems 1 & 2). Detailed computations for the examples of stabilizing policies in Figure 3 can be found in (Tang et al., 2023, Example 11). Quotient spaces of linear systems are first studied by Kalman and Hazelwinkel, known as geometric linear system theory, in the early 1970s (Hazewinkel and

Kalman, 1976; Hazewinkel, 1980). This perspective focuses on the state-space forms of systems and their algebraic-geometric properties under the feedback. Herein, we focus on the space of stabilizing policies and their symmetries under similarity transformations. The (KM) Riemannian metric is introduced in (Kraisler and Mesbahi, 2024), differing slightly from the KM metric in (Krishnaprasad and Martin, 1983) and studied in (Afsari and Vidal, 2017). Theorem 3.3 is proved in (Kraisler and Mesbahi, 2024, Thm. 3.2). For abstract quotient spaces and smooth quotient manifold conditions, see (Lee, 2010, §21).

In §4, Lemma 4.1 is reviewed from (Talebi and Mesbahi, 2023, Lemma 4.1). Hewer’s algorithm in Remark 1 is introduced in (Hewer, 1971). The properties of J_{LQR} in Lemma 4.3 are studied in (Fazel et al., 2018a; Bu et al., 2019; Talebi and Mesbahi, 2023), with similar properties for Mean-squared error in state estimation in (Talebi et al., 2023). The results of §4.4 are adapted from (Tang et al., 2023; Kraisler and Mesbahi, 2024; Zheng et al., 2022), with related developments in (Hu and Zheng, 2022; Zheng et al., 2023; Umenberger et al., 2022; Zhang et al., 2023). Facts 4.2 and 4.3 are adapted from (Tang et al., 2023, Theorem 5 and 6). Fact 4.4 is formally proved in (Kraisler and Mesbahi, 2024, Lem 5.3). For the KYP lemma, see (Rantzer, 1996), and for G -invariant metrics and G -equivariance retraction, see (Boumal, 2023, Sect. 9.9).

Lemma 4.5 aggregates results from various resources. The non-smoothness of \mathcal{H}_∞ cost is in (Apkarian and Noll, 2006a,b), with subdifferential regularity from (Clarke, 1990). Recent discussions are in (Guo and Hu, 2022, Proposition 2), (Tang and Zheng, 2023, Proposition 1), with coercivity in (Guo and Hu, 2022, Lemma 1) and connectivity of sublevel sets in (Guo and Hu, 2022, Lemma 2) and (Hu and Zheng, 2022). The subdifferentials of the \mathcal{H}_∞ cost function are computed in (Zheng et al., 2023, Lemma 5.2). Fact 4.5 is first proved in (Guo and Hu, 2022, Theorem 1) for discrete-time dynamics, with the continuous-time state-feedback \mathcal{H}_∞ control counterpart in (Zheng et al., 2024, Corollary 4.1). At the time of writing, geometrical properties for output-feedback \mathcal{H}_∞ control are under active investigation; see e.g., (Zheng et al., 2023; Tang and Zheng, 2023; Guo et al., 2024).

In addition to the state-feedback \mathcal{H}_∞ control, some recent studies have also investigated policy optimization in other control problems with robustness features. For example, policy optimization for linear risk-sensitivity control and a general mixed $\mathcal{H}_2/\mathcal{H}_\infty$ is studied in Zhang et al. (2020), where a notion of implicit regularization is introduced to deal with the challenge of lacking coerciveness in the mixed design. Model-free μ -synthesis was studied in Keivan et al. (2022) and global convergences for risk-constrained LQR are recently investigated in Zhao et al. (2023). In the realm of data-driven policy optimization algorithms, notable methods include REINFORCE Williams (1992) and Proximal Policy Optimization (PPO) Schulman et al. (2017) which operate within the context of Markov Decision Processes (MDPs), leveraging the finiteness of state and action domains. They estimate the gradient by using the likelihood ratio method Sutton et al. (1999).

8. Acknowledgements

S. Talebi and N. Li are partially supported by NSF AI institute 2112085. Y. Zheng is supported in part by NSF ECCS-2154650 and NSF CAREER 2340713. S. Kraisler and M. Mesbahi have been supported by NSF grant ECCS-2149470 and AFOSR grant FA9550-20-1-0053.

References

Ackermann, J., 1980. Parameter space design of robust control systems. IEEE Transactions on Automatic Control 25, 1058–1072. doi:10.1109/TAC.1980.1102505.

- Afsari, B., Vidal, R., 2017. Bundle Reduction and the Alignment Distance on Spaces of State-Space LTI Systems. *IEEE Transactions on Automatic Control* 62, 3804–3819. URL: <http://ieeexplore.ieee.org/document/7872404/>, doi:10.1109/TAC.2017.2678839.
- Agarwal, A., Kakade, S.M., Lee, J.D., Mahajan, G., 2021. On the theory of policy gradient methods: optimality, approximation, and distribution shift. *J. Mach. Learn. Res.* 22, 4431–4506.
- Alemzadeh, S., Talebi, S., Mesbahi, M., 2024. Data-Driven Structured Policy Iteration for Homogeneous Distributed Systems. *IEEE Transactions on Automatic Control* , 1–15URL: <https://ieeexplore.ieee.org/abstract/document/10436325>, doi:10.1109/TAC.2024.3366038. conference Name: *IEEE Transactions on Automatic Control*.
- Amari, S.i., 1998. Natural Gradient Works Efficiently in Learning. *Neural Computation* 10, 251–276. URL: <https://doi.org/10.1162/089976698300017746>, doi:10.1162/089976698300017746.
- Amari, S.I., 2016. *Information Geometry and Its Applications*. Springer.
- Anderson, B.D., Moore, J.B., 2007. *Optimal control: linear quadratic methods*. Courier Corporation.
- Apkarian, P., Noll, D., 2006a. Nonsmooth H_∞ synthesis. *IEEE Transactions on Automatic Control* 51, 71–86.
- Apkarian, P., Noll, D., 2006b. Nonsmooth optimization for multidisk H_∞ synthesis. *European Journal of Control* 12, 229–244.
- Åström, K.J., Murray, R., 2021. *Feedback systems: an introduction for scientists and engineers*. Princeton university press.
- Bertsekas, D., 2012. *Dynamic Programming and Optimal Control: Volume I*. Athena Scientific.
- Bertsekas, D.P., 2011. Approximate policy iteration: a survey and some new methods. *J. Control Theory Appl.* 9, 310–335.
- Bertsekas, D.P., 2017. Value and policy iterations in optimal control and adaptive dynamic programming. *IEEE Trans. Neural Netw. Learn. Syst.* 28, 500–509.
- Boumal, N., 2023. *An introduction to optimization on smooth manifolds*. Cambridge University Press, Cambridge ; New York, NY.
- Boyd, S., El Ghaoui, L., Feron, E., Balakrishnan, V., 1994. *Linear Matrix Inequalities in System and Control Theory*. Society for Industrial and Applied Mathematics.
- Bradtke, S., Ydstie, B., Barto, A., 1994. Adaptive linear quadratic control using policy iteration, in: *Proceedings of 1994 American Control Conference - ACC '94*, IEEE, Baltimore, MD, USA. pp. 3475–3479. URL: <http://ieeexplore.ieee.org/document/735224/>, doi:10.1109/ACC.1994.735224.
- Brockett, R., 2014. The early days of geometric nonlinear control. *Automatica* 50, 2203–2224.

- Bu, J., Mesbahi, A., Fazel, M., Mesbahi, M., 2019. LQR through the Lens of First Order Methods: Discrete-time Case. URL: <http://arxiv.org/abs/1907.08921>, doi:10.48550/arXiv.1907.08921. arXiv:1907.08921 [cs, eess, math].
- Bu, J., Mesbahi, A., Mesbahi, M., 2021. On Topological Properties of the Set of Stabilizing Feedback Gains. IEEE Transactions on Automatic Control 66, 730–744. URL: <https://ieeexplore.ieee.org/abstract/document/9086139>, doi:10.1109/TAC.2020.2992510. conference Name: IEEE Transactions on Automatic Control.
- Chang, T.J., Shahrapour, S., 2024. Regret Analysis of Policy Optimization over Submanifolds for Linearly Constrained Online LQG. URL: <http://arxiv.org/abs/2403.08553>. arXiv:2403.08553 [cs, eess, math].
- Clarke, F.H., 1990. Optimization and Nonsmooth Analysis. Society for Industrial and Applied Mathematics.
- Doyle, J.C., Francis, B.A., Tannenbaum, A.R., 2013. Feedback Control Theory. Courier Corporation.
- Duan, J., Cao, W., Zheng, Y., Zhao, L., 2024. On the optimization landscape of dynamic output feedback linear quadratic control. IEEE Transactions on Automatic Control 69, 920–935. doi:10.1109/TAC.2023.3275732.
- Fam, A., Meditch, J., 1978. A canonical parameter space for linear systems design. IEEE Transactions on Automatic Control 23, 454–458.
- Fazel, M., Ge, R., Kakade, S., Mesbahi, M., 2018a. Global convergence of policy gradient methods for the linear quadratic regulator, in: International conference on machine learning, PMLR. pp. 1467–1476.
- Fazel, M., Ge, R., Kakade, S.M., Mesbahi, M., 2018b. Global convergence of policy gradient methods for the linear quadratic regulator, in: Proceedings of the 35th International Conference on Machine Learning.
- Feng, H., Lavaei, J., 2019. On the Exponential Number of Connected Components for the Feasible Set of Optimal Decentralized Control Problems, in: 2019 American Control Conference (ACC), pp. 1430–1437. doi:10.23919/ACC.2019.8814952.
- Flaxman, A.D., Kalai, A.T., McMahan, H.B., 2004. Online convex optimization in the bandit setting: gradient descent without a gradient. URL: <http://arxiv.org/abs/cs/0408007>. arXiv:cs/0408007.
- Grondman, I., Busoniu, L., Lopes, G.A.D., Babuška, R., . A Survey of Actor-Critic Reinforcement Learning: Standard and Natural Policy Gradients .
- Guo, X., Hu, B., 2022. Global convergence of direct policy search for state-feedback \mathcal{H}_∞ robust control: A revisit of nonsmooth synthesis with Goldstein subdifferential, in: Advances in Neural Information Processing Systems, Curran Associates, Inc.. pp. 32801–32815.
- Guo, X., Keivan, D., Dullerud, G., Seiler, P., Hu, B., 2024. Complexity of derivative-free policy optimization for structured \mathcal{H}_∞ control. Advances in Neural Information Processing Systems 36.

- Hazewinkel, M., 1976. Moduli and canonical forms for linear dynamical systems II: The topological case. *Mathematical Systems Theory* 10, 363–385. URL: <http://link.springer.com/10.1007/BF01683285>, doi:10.1007/BF01683285.
- Hazewinkel, M., 1980. (Fine) Moduli (Spaces) for Linear Systems: What are they and what are they Good for?, in: Byrnes, C.I., Martin, C.F. (Eds.), *Geometrical Methods for the Theory of Linear Systems*. Springer Netherlands, Dordrecht, pp. 125–193. URL: http://link.springer.com/10.1007/978-94-009-9082-1_3, doi:10.1007/978-94-009-9082-1_3.
- Hazewinkel, M., Kalman, R.E., 1976. On Invariants, Canonical Forms and Moduli for Linear, Constant, Finite Dimensional, Dynamical Systems, in: Beckmann, M., Künzi, H.P., Marchesini, G., Mitter, S.K. (Eds.), *Mathematical Systems Theory*. Springer Berlin Heidelberg, Berlin, Heidelberg. volume 131, pp. 48–60. URL: http://link.springer.com/10.1007/978-3-642-48895-5_4, doi:10.1007/978-3-642-48895-5_4.
- Hewer, G., 1971. An iterative technique for the computation of the steady state gains for the discrete optimal regulator. *IEEE Transactions on Automatic Control* 16, 382–384. URL: <https://ieeexplore.ieee.org/document/1099755>, doi:10.1109/TAC.1971.1099755. conference Name: IEEE Transactions on Automatic Control.
- Hu, B., Zhang, K., Li, N., Mesbahi, M., Fazel, M., Başar, T., 2023. Toward a theoretical foundation of policy optimization for learning control policies. *Annual Review of Control, Robotics, and Autonomous Systems* 6, 123–158.
- Hu, B., Zheng, Y., 2022. Connectivity of the feasible and sublevel sets of dynamic output feedback control with robustness constraints. *IEEE Control Systems Letters* 7, 442–447.
- Hyland, D., Bernstein, D., 1984. The optimal projection equations for fixed-order dynamic compensation. *IEEE Transactions on Automatic Control* 29, 1034–1037.
- Isidori, A., 2013. *Nonlinear Control Systems*. Springer Science & Business Media.
- Jin, C., Ge, R., Netrapalli, P., Kakade, S.M., Jordan, M.I., 2017. How to escape saddle points efficiently, in: *International conference on machine learning*, PMLR. pp. 1724–1732.
- Jury, E.I., 1964. *Theory and application of the z-transform method* .
- Kakade, S.M., 2001. A Natural Policy Gradient, in: *Advances in Neural Information Processing Systems*, MIT Press. URL: https://proceedings.neurips.cc/paper_files/paper/2001/hash/4b86abe48d358ecf194c56c69108433e-Abstract.html.
- Kakade, S.M., 2002. A natural policy gradient, in: Dietterich, T.G., Becker, S., Ghahramani, Z. (Eds.), *Advances in Neural Information Processing Systems* 14. MIT Press, pp. 1531–1538.
- Keivan, D., Havens, A., Seiler, P., Dullerud, G., Hu, B., 2022. Model-free μ synthesis via adversarial reinforcement learning, in: *2022 American Control Conference (ACC)*, IEEE. pp. 3335–3341.
- Kraisler, S., Mesbahi, M., 2024. Output-feedback synthesis orbit geometry: Quotient manifolds and lqg direct policy optimization. arXiv preprint arXiv:2403.17157 .
- Krishnaprasad, P.S., Martin, C.F., 1983. On families of systems and deformations. *International Journal of Control* 38, 1055–1079.

- Lee, J., 2010. Introduction to Topological Manifolds. 2nd ed., Springer Science & Business Media.
- Lee, J.M., 2018. Introduction to Riemannian Manifolds. 2nd ed., Cham, Switzerland: Springer Nature.
- Lewis, A.S., 2007. Nonsmooth optimization and robust control. *Annual Reviews in Control* 31, 167–177.
- Liberzon, D., 2011. Calculus of Variations and Optimal Control Theory: A Concise Introduction. Princeton University Press.
- Malik, D., Pananjady, A., Bhatia, K., Khamaru, K., Bartlett, P., Wainwright, M., 2019. Derivative-Free methods for policy optimization: Guarantees for linear quadratic systems, in: Chaudhuri, K., Sugiyama, M. (Eds.), *Proceedings of the Twenty-Second International Conference on Artificial Intelligence and Statistics*, PMLR. pp. 2916–2925.
- Mohammadi, H., Soltanolkotabi, M., Jovanovic, M.R., 2020. Random search for learning the linear quadratic regulator, in: *2020 American Control Conference (ACC)*, IEEE. pp. 4798–4803.
- Mohammadi, H., Soltanolkotabi, M., Jovanović, M.R., 2021a. Model-Free linear quadratic regulator, in: Vamvoudakis, K.G., Wan, Y., Lewis, F.L., Cansever, D. (Eds.), *Handbook of Reinforcement Learning and Control*. Springer International Publishing, Cham, pp. 173–185.
- Mohammadi, H., Soltanolkotabi, M., Jovanović, M.R., 2021b. On the lack of gradient domination for linear quadratic gaussian problems with incomplete state information, in: *2021 60th IEEE Conference on Decision and Control (CDC)*, IEEE. pp. 1120–1124.
- Mohammadi, H., Zare, A., Soltanolkotabi, M., Jovanović, M.R., 2021c. Convergence and sample complexity of gradient methods for the model-free linear–quadratic regulator problem. *IEEE Transactions on Automatic Control* 67, 2435–2450.
- Nijmeijer, H., Schaft, A., 1990. *Nonlinear Dynamical Control Systems*. Springer New York.
- Ober, R.J., 1987. Topology of the set of asymptotically stable minimal systems. *International Journal of Control* 46, 263–280.
- Ohara, A., Amari, S.i., 1992a. Differential geometric structures of stable state feedback systems with dual connections. *IFAC Proceedings Volumes* 25, 176–179.
- Ohara, A., Amari, S.I., 1992b. Differential Geometric Structures of Stable State Feedback Systems with Dual Connections. *IFAC Proceedings* 25, 176–179. URL: <https://www.sciencedirect.com/science/article/pii/S147466701749745X>, doi:[https://doi.org/10.1016/S1474-6670\(17\)49745-X](https://doi.org/10.1016/S1474-6670(17)49745-X).
- Parks, P.C., 1962. A new proof of the Routh-Hurwitz stability criterion using the second method of liapunov, in: *Mathematical Proceedings of the Cambridge Philosophical Society*, Cambridge University Press. pp. 694–702.
- Rantzer, A., 1996. On the Kalman–Yakubovich–Popov lemma. *Systems & Control Letters* 28, 7–10.

- Recht, B., 2019. A tour of reinforcement learning: The view from continuous control. Annual Review of Control, Robotics, and Autonomous Systems 2, 253–279.
- Schulman, J., Wolski, F., Dhariwal, P., Radford, A., Klimov, O., 2017. Proximal Policy Optimization Algorithms. URL: <http://arxiv.org/abs/1707.06347>. arXiv:1707.06347 [cs].
- Skogestad, S., Postlethwaite, I., 2005. Multivariable Feedback Control: Analysis and Design. John Wiley & Sons.
- Sontag, E.D., 2013. Mathematical Control Theory: Deterministic Finite Dimensional Systems. Springer Science & Business Media.
- Spall, J.C., 1998. An Overview of the Simultaneous Perturbation Method. JOHNS HOPKINS APL TECHNICAL DIGEST 19.
- Sutton, R.S., McAllester, D., Singh, S., Mansour, Y., 1999. Policy Gradient Methods for Reinforcement Learning with Function Approximation, in: Advances in Neural Information Processing Systems, MIT Press. URL: <https://proceedings.neurips.cc/paper/1999/hash/464d828b85b0bed98e80ade0a5c43b0f-Abstract.html>.
- Takakura, S., Sato, K., 2024. Structured Output Feedback Control for Linear Quadratic Regulator Using Policy Gradient Method. IEEE Transactions on Automatic Control 69, 363–370. URL: <https://ieeexplore.ieee.org/document/10091214/>, doi:10.1109/TAC.2023.3264176.
- Talebi, S., Alemzadeh, S., Rahimi, N., Mesbahi, M., 2022. On Regularizability and Its Application to Online Control of Unstable LTI Systems. IEEE Transactions on Automatic Control 67, 6413–6428. URL: <https://ieeexplore.ieee.org/abstract/document/9627635>, doi:10.1109/TAC.2021.3131148. conference Name: IEEE Transactions on Automatic Control.
- Talebi, S., Mesbahi, M., 2022. Riemannian Constrained Policy Optimization via Geometric Stability Certificates, in: 2022 IEEE 61st Conference on Decision and Control (CDC), pp. 1472–1478. doi:10.1109/CDC51059.2022.9992877.
- Talebi, S., Mesbahi, M., 2023. Policy Optimization over Submanifolds for Linearly Constrained Feedback Synthesis. IEEE Transactions on Automatic Control , 1–16URL: <https://ieeexplore.ieee.org/document/10224332>, doi:10.1109/TAC.2023.3306384. conference Name: IEEE Transactions on Automatic Control.
- Talebi, S., Taghvaei, A., Mesbahi, M., 2023. Data-driven Optimal Filtering for Linear Systems with Unknown Noise Covariances. Advances in Neural Information Processing Systems 36, 69546–69585. URL: https://proceedings.neurips.cc/paper_files/paper/2023/hash/dbe8185809cb7032ec7ec6e365e3ed3b-Abstract-Conference.html.
- Tang, Y., Zheng, Y., 2023. On the global optimality of direct policy search for nonsmooth \mathcal{H}_∞ output-feedback control, in: 2023 62nd IEEE Conference on Decision and Control (CDC), IEEE. pp. 6148–6153.
- Tang, Y., Zheng, Y., Li, N., 2023. Analysis of the optimization landscape of linear quadratic gaussian (lqg) control. Mathematical Programming 202, 399–444.
- Tannenbaum, A.R., 1981. Invariance and system theory: algebraic and geometric aspects. Number 845 in Lecture notes in mathematics, Springer, Berlin.

- Trentelman, H.L., Stoorvogel, A.A., Hautus, M., 2001. Control theory for linear systems.
- Umenberger, J., Simchowitz, M., Perdomo, J., Zhang, K., Tedrake, R., 2022. Globally convergent policy search for output estimation. *Advances in Neural Information Processing Systems* 35, 22778–22790.
- Williams, R.J., 1992. Simple statistical gradient-following algorithms for connectionist reinforcement learning. *Machine Learning* 8, 229–256. URL: <https://doi.org/10.1007/BF00992696>, doi:10.1007/BF00992696.
- Wonham, W.M., 1985. *Linear Multivariable Control*. Springer Science+Business Media, LLC, New York. URL: <https://link-springer-com.ezp-prod1.hul.harvard.edu/book/10.1007/978-1-4612-1082-5>.
- Yu, J., Gupta, V., Wierman, A., 2023. Online Stabilization of Unknown Linear Time-Varying Systems. URL: <https://arxiv.org/abs/2304.02878v2>.
- Zabczyk, J., 2020. *Mathematical Control Theory*. Birkhäuser.
- Zhang, K., Hu, B., Basar, T., 2020. Policy optimization for \mathcal{H}_2 linear control with \mathcal{H}_∞ robustness guarantee: Implicit regularization and global convergence, in: *Learning for Dynamics and Control*, PMLR. pp. 179–190.
- Zhang, X., Hu, B., Başar, T., 2023. Learning the kalman filter with fine-grained sample complexity, in: *2023 American Control Conference (ACC)*, IEEE. pp. 4549–4554.
- Zhao, F., You, K., Başar, T., 2023. Global convergence of policy gradient primal-dual methods for risk-constrained lqrs. *IEEE Transactions on Automatic Control* .
- Zheng, Y., Pai, C.f., Tang, Y., 2023. Benign nonconvex landscapes in optimal and robust control, Part I: Global optimality. *arXiv preprint arXiv:2312.15332* .
- Zheng, Y., Pai, C.f., Tang, Y., 2024. Benign nonconvex landscapes in optimal and robust control, Part II: Extended convex lifting. *preprint* .
- Zheng, Y., Sun, Y., Fazel, M., Li, N., 2022. Escaping high-order saddles in policy optimization for linear quadratic gaussian (lqg) control, in: *2022 IEEE 61st Conference on Decision and Control (CDC)*, IEEE. pp. 5329–5334.
- Zhou, K., Doyle, J.C., Glover, K., 1996. *Robust and Optimal Control*. Prentice Hall.
- Zhou, K., Khargonekar, P.P., 1988. An algebraic riccati equation approach to \mathcal{H}_∞ optimization. *Systems & Control Letters* 11, 85–91.